Characterization of target genes at the 2p15–16 amplicon in diffuse large B-cell lymphoma

Noriko Fukuhara,[1,2] Hiroyuki Tagawa,[1] Yoshihiro Kameoka,[1] Yumiko Kasugai,[1] Sivasundaram Karnan,[1] Junichi Kameoka,[2] Takeshi Sasaki,[2] Yasuo Morishima,[3] Shigeo Nakamura[4] and Masao Seto[1,5]

[1]Division of Molecular Medicine, Aichi Cancer Center Research Institute, Nagoya 464-8681, [2]Department of Rheumatology and Hematology, Tohoku University School of Medicine, Sendai 980-8574, [3]Department of Hematology and Cell Therapy, Aichi Cancer Center Hospital, Nagoya 464-8681, [4]Pathology/Clinical Laboratories, Nagoya University Hospital, Nagoya 466-8550, Japan

(Received November 4, 2005/Revised January 26, 2006/Accepted February 20, 2006/Online publication May 11, 2006)

Amplification of 2p has been observed as a recurrent alteration in diffuse large B-cell lymphoma (DLBCL). Whereas two candidate oncogenes, *REL and BCL11A*, have been investigated as targets for 2p amplification, the question remains as to whether the true target gene in the amplicon is *REL*, *BCL11A* or both. We previously identified frequent genomic gains of chromosomal 2p in 25 out of 99 DLBCL cases by means of genome-wide array comparative genomic hybridization (CGH). All of these 25 cases included recurrent copy number gain at 2p15–16. In the study presented here, cases were analyzed in greater detail by means of contig bacterial artificial chromosome (BAC) array CGH for the 4.5-Mb region at 2p15–16, which contained 33 BAC clones. We confined the minimal common region to 500-kb in length, where only the candidate oncogene *REL*, and not *BCL11A*, is located. Real-time quantitative PCR was carried out to investigate the correlation between genomic gain and expression. It showed a significant correlation for both genes, indicating that these two genes are common targets for the 2p15–16 amplicon. However, given the fact that *REL* is more frequently amplified than *BCL11A*, the *REL* gene may play a more important role than *BCL11A* in the pathogenesis of DLBCL. (*Cancer Sci* 2006; 97: 499–504)

Diffuse large B cell lymphoma (DLBCL) is the most common type of malignant lymphoma, accounting for 30% of adult non-Hodgkin's lymphoma.[1] However, clinicopathological and genetic heterogeneities in this entity have suggested that further refinement of its subgroups is required.[2–5] Array-based comparative genomic hybridization (array-CGH) analysis is a powerful tool to identify genomic imbalances characteristic of distinct subgroups in DLBCL.[6,7] It has been useful not only for genome scanning of tumor cells but also for identification of novel oncogenes and suppressor genes.[8]

We previously used a genome-wide array-CGH to identify a gain of 2p15–16 in 25 out of 99 DLBCL cases.[7] Amplification at the 2p arm has been reported in B-cell lymphomas, such as DLBCL,[9–15] classical Hodgkin's lymphoma (cHL),[16,17] follicular lymphoma (FL)[18] and primary mediastinal B-cell lymphoma (PMBCL).[11,14,15] The two candidate genes, *REL* and *BCL11A*, have been mapped within this 2p15–16 amplicon. The *REL* proto-oncogene, which encodes a member of the NF-κB transcription factor family, has frequently been found amplified in B-cell lymphomas. *BCL11A*, which is located quite near *REL* on chromosome 2p15–16, is coamplified with *REL* in DLBCL and cHL.[12,15,16] In spite of numerous studies of this region, the question remains whether the target gene in the 2p15–16 amplification is *REL*, *BCL11A*, or both.

For the study presented here, we carried out a contig array-CGH using glass slides on which contiguously ordered bacterial artificial chromosome (BAC) clones were spotted throughout 4.5 Mb of the 2p15–16 genome to confine the minimal common region of amplification at 2p15–16 in DLBCL cases. Real-time quantitative-polymerase chain reaction (RQ-PCR) analysis was then used to further investigate the relationship between genomic amplification and expression.

Patients, Materials and Methods

Tumor samples

Tumor samples were obtained from 99 patients under a protocol approved by the International Review Board of the Aichi Cancer Center. Informed consent was obtained in accordance with the Declaration of Helsinki. All of the DNA and RNA samples were obtained from tumors at the time of diagnosis before the administration of any treatment. DNA was extracted with a standard phenol chloroform method from lymphoma specimens of the tumors. Normal DNA was prepared from peripheral-blood lymphocytes of healthy male donors. Total RNA was extracted using the standardized guanidium isothiocyanate and cecium chloride method from lymphoma specimens taken from the tumors. Data for genomic gains and losses at the chromosome 2 region of the 99 DLBCL have been reported previously.[7]

Genome-wide array-based CGH

DNA preparation, labeling, array fabrication and hybridization were carried out as described elsewhere.[6,8,19] Briefly, the array consisted of 2213 BAC and P-1-derived artificial chromosome (PAC) clones, covering the whole human genome with a resolution of 1.3 Mb, from library RP11, 13 for BAC clones and RP1, and 3, 4, 5 for PAC clones. Of the 2213 clones spotted on the glass slides, 188 were of chromosome 2, and of these 188 BAC/PAC clones, 75 were of the short arm of chromosome 2 (2p). These clones were obtained from the BAC/PAC Resource Center at the Children's Hospital Oakland Research Institute, Oakland,

[5]To whom correspondence should be addressed. E-mail: mseto@aichi-cc.jp

doi: 10.1111/j.1349-7006.2006.00209.x

CA, USA (http://bacpac.chori.org/). The thresholds for the $\log_2$ ratio of gains and losses were set at the $\log_2$ ratios of +0.2 and −0.2, respectively. High-level copy number gain (amplification) was defined as $\log_2$ ratio ≥ +1 and low-level copy number gain as $+0.2 \leq \log_2$ ratio < +1.0.[8]

Contig array-based CGH

Detailed analysis with contig array-CGH was carried out for cases with amplification ($n = 3$) and gain ($n = 4$, cases with available RNA and restricted region of gain) at 2p15–16. Selection of 33 BAC clones of 2p15–16 was based on information from National Center of Biotechnology Information (NCBI) (http://www.ncbi.nlm.nih.gov/). Each clone was placed contiguously between BAC clones RP11–518G12 and RP11–511I11 according to the mapping position obtained from the NCBI. These clones were obtained from the BAC/PAC Resource Center at the Children's Hospital Oakland Research Institute. BAC were then isolated from their bacterial cultures with the relevant antibiotics and extracted with a plasmid Mini-Kit (Qiagen, Valencia, CA, USA). The exact location of each clone was determined by means of standard fluorescence in site hybridization (FISH) analysis. Degenerate oligonucleotide-primed polymerase chain reaction (DOP-PCR)[20] was carried out on the DNA of BAC clones, as described elsewhere.[8] DOP-PCR products were dissolved in 30 μL of TE (100 mM Tris-HCl and 1 mM ethylenediaminetetracetic acid, pH 7.5) buffer, and 10 μL of Solution I (Takara Bio, Tokyo, Japan) was added to each of the products, which were then spotted in triplicate onto Hubble-activated slides (Takara Bio) using the Stampman Arrayer (Nippon Laser and Electronics Laboratory, Nagoya, Japan) with a split pin. Slides were fixed in 0.2% sodium dodecylsulfate for 2 min and in 0.3 M NaOH for 5 min, then dehydrated with 100% cold ethanol for 3 min, and finally air-dried. DNA preparation, labeling, array fabrication and hybridization were carried out according to methods described previously.[6,8,21,22] The Agilent Micro Array Scanner (Agilent Technologies, Palo Alto, CA, USA) was used for scanning analysis. The array images thus acquired were further analyzed with Genepix Pro 4.1 (Axon Instruments, Foster City, CA, USA).

Reverse transcription–polymerase chain reaction analysis for screening of candidate genes

The RC-K8 cell line was established from histiocytic lymphoma cells (kindly provided by I. Kubonishi, Kochi, Japan).[23] The L428 cell line was established from Hodgkin's lymphoma (German Collection of Microorganisms and Cell Cultures, Braunschweig, Germany).[24] The Karpas-1106p cell line was established from mediastinal lymphoblastic B-cell lymphoma (kindly provided by A. Karpas, Cambridge, UK).[25] These cell lines and human placenta[26] were subjected to reverse transcription–polymerase chain reaction (RT-PCR) analysis. SuperScript II (Gibco-BRL, Gaithersburg, MD, USA) was used for cDNA. Each 5 μg of total RNA was reverse-transcribed into cDNA in a volume of 40 μL distilled water. RT-PCR was carried out for nine genes by using the specific corresponding primers. The names and accession numbers of the genes were: *LOC442017* (XM_497839), *LOC130865* (XM_497840), *ATP1B3P1* (NG_000849), *PAPOLG* (NM_022894), *LOC400957* (XM_379097), *REL* (NM_002908), *LOC344423* (AK124741), *FLJ32312* (NM_144709) and *PEX13* (NM_002618). The primers used for RT-PCR are shown in Table 1. Each primer was designed so that the melting temperature (Tm) value would be between 58°C and 63°C. Amplifications were carried out using a Thermal Cycler (Perkin-Elmer, Norwalk, CT, USA), and RT-PCR was carried out using the touchdown PCR method. The reactions comprised 10 cycles of denaturation (94°C, 0.5 min), annealing (65°C, 0.5 min, 1°C decrease per 2 cycles) and extension (72°C, 2.5 min), followed by 35 cycles of denaturation (94°C, 0.5 min), annealing (60°C, 0.5 min) and extension (72°C, 2.5 min), and a final extension of 5 min at 72°C. In the cases of *LOC130865* and *LOC442017*, annealing temperature of the reaction ranged from 63 to 58°C.

Real-time quantitative–polymerase chain reaction

Expression levels of *REL*, *BCL11A*, *LOC344423* and *PEX13* mRNA were measured by means of real-time fluorescence detection using a previously described method.[22,27] Briefly, the primers of *REL* were sense: 5′-cccacgctcaggcaataca-3′ and antisense: 5′-tggtgggataccttgcgaat-3′, those of *BCL11A* were sense: 5′-aaaaagagagaaacaaaaaagtgtgaca-3′ and antisense: 5′-catccatgtgacattctagcagg-3′, those of *LOC344423* were sense: 5′- gccatgcactagagggtactca-3′ and antisense: 5′-gctcttcttgacacctcatcaa-3′, and those of *PEX13* were sense: 5′-aggaccgagcagctacctca-3′ and antisense: 5′-tggcaa-ctacatggtcatcctc-3′. Real-time PCR using SYBR® Green1 and primers was carried out with a Smart Cycler System (Takara Bio) according to the manufacturer's protocol. *G6PDH* served as an endogenous control, whereas the expression

Table 1. Reverse transcription–polymerase chain reaction analysis of genes within the 2p15–16 amplification region of RC-K8, L428 and Karpas-1106p

Gene	Forward primer	Reverse primer	Human placenta	RC-K8	L428	Karpas 1106p
LOC442017	5′-ctgtccaaaccgtcttcactc	5′-acttggcagtggaggcgtag	+/–	–	–	+/–
LOC130865	5′-cccacactcgcagaaagatt	5′-acagggacagctatgctgttag	+/–	+/–	+/–	+
ATP1B3P1	5′-gcacacgatgaagaaggagtc	5′-gcttgaagtaacgaaatgggagat	+/–	+/–	+/–	–
PAPOLG	5′-attgacgccatgaaaccatt	5′-gcttctcaggcgagagtcgt	+	+	+	–
LOC400957	5′-actatagccggatacagggaga	5′-cgtagcacccgttacacaga	+/–	+	+/–	–
REL	5′-gaaactgtgccaggatcacg	5′-ccaacaggtattctcaggaatgg	+	++	++	++
LOC344423	5′-catgatggcctagcatatgaa	5′-gctcttcttgacacctcatcaa	+	++	++	++
FLJ32312	5′-tctgttagtcatgttggaagcact	5′-ggctttcataactgccattcta	+/–	–	+	+
PEX13	5′-acaaccgcctccgtgtaga	5′-ctctggcaactacatggtcatc	+	++	++	++

Detected by electrohphoresis: ++, positive thick band; +, positive thin band; +/–, very weakly positive band; –, no band.

doi: 10.1111/j.1349-7006.2006.00209.x

levels of *REL*, *BCL11A*, *LOC344423* and *PEX13* mRNA in each sample were normalized on the basis of the corresponding *G6PDH* content and recorded as relative expression levels. Overexpression was defined as the mean of the relative expression plus two or more standard deviation units.

Results

Recurrent amplification detected by genome-wide array-CGH at 2p15–16 in DLBCL

Genome-wide array-CGH analysis at a resolution of 1.3 Mb showed that 25 of the 99 DLBCL cases (25%) had copy number gains on chromosome 2p. All cases included recurrent copy number gain at 2p15–16, with three of the 25 cases showing genomic amplification ($\log_2$ ratio ≥ 1). Individual genomic profiles of these three tumors (D768, D778 and D792) showed that every amplification was located at 2p15–16 (Fig. 1). The common recurrent region of the 25 cases was confined to the 4.5-Mb region at 2p15–16 (Fig. 2).

Determination of minimal common region by contig array-CGH

We speculated that the target genes of 2p15–16 amplification were located within the common recurrent region between BAC clones RP11–518G12 and RP11–511I11. To specify the alterations of 2p15–16 in more detail, we prepared high-resolution contig array glass slides containing 33 BAC clones, which were placed contiguously throughout the 4.5-Mb region. Contig array-CGH was conducted for seven cases, for which the genome-wide array-CGH showed gain or amplification at 2p15–16 (Fig. 3). The profiles showed that the common region for three cases with amplification ($\log_2$ ratio ≥ 1.0) was 1.6 Mb located between BAC clones RP11–440P5 and RP11–813L21. Further analysis for four cases with genomic gain confined the minimal common region to 500 kb between BAC clones RP11–416L21 and RP11–373L24. The region contained only *REL*, not *BCL11A*, as the candidate oncogene.

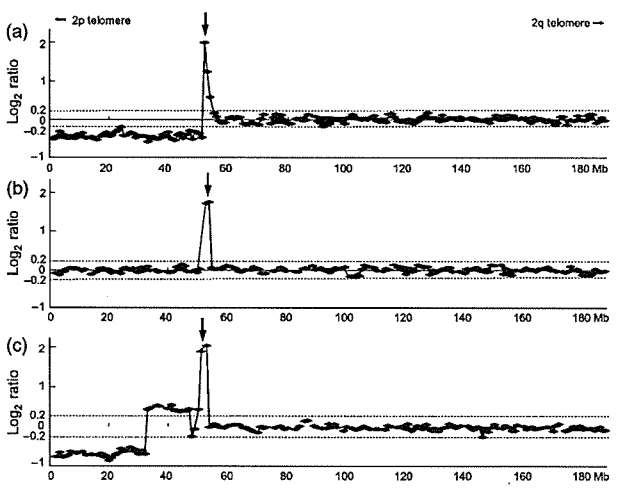

Fig. 1. Representative individual genomic profiles of chromosome 2 in diffuse large B-cell lymphoma. Genome-wide array-based comparative genomic hybridization profiles of three cases with 2p amplification: (a) D768, (b) D778 and (c) D792. Dots represent the $\log_2$ ratio of bacterial artificial chromosome/P-1-derived artificial chromosome clones, which are shown in order from the p telomere to the q telomere. The vertical arrow above each profile indicates the region of amplification. The threshold for gain and loss was defined as the $\log_2$ ratio of +0.2 and −0.2, respectively.

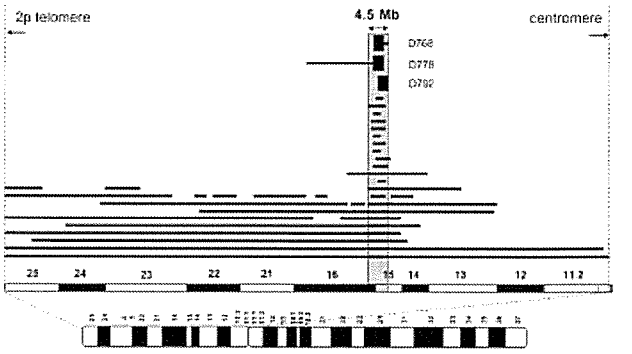

Fig. 2. Illustration of genomic amplification at chromosome 2p. Summary of genome-wide array-based comparative genomic hybridization profiles at 2p. Copy number gains were detected in 25 of 99 diffuse large B-cell lymphoma cases. Thin lines: low copy number gain (+0.2 ≤ $\log_2$ ratio < +1.0); thick lines: high copy number gain (amplification, $\log_2$ ratio ≥ +1.0). Genomic amplifications were observed at 2p15–16 in three cases (D768, D778 and D792). The gray area represents the most common recurrent region in the 25 cases, which is 4.5 Mb in length.

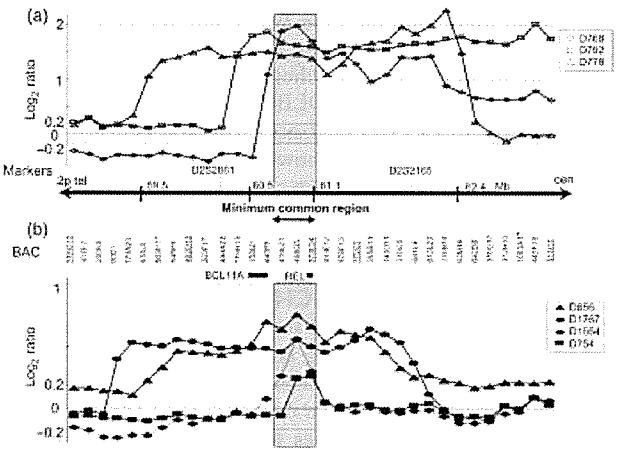

Fig. 3. Contig array-based comparative genomic hybridization (array-CGH) profiles at 2p15–16 in diffuse large B-cell lymphoma. Contig array-CGH containing 33 bacterial artificial chromosome (BAC) clones were constructed and placed contiguously at the most common recurrent region (4.5 Mb) identified with genome-wide array-CGH. (a) Genomic profiles of three cases with high copy number gain ($\log_2$ ratio ≥ +1.0) at 2p15–16. (b) Genomic profiles for four cases with low copy number gain (+ 0.2 ≤ $\log_2$ ratio < +1.0) at 2p15–16. Dots represent the $\log_2$ ratio of BAC clones, which are shown in order from the p telomere to the centromere. Vertical lines: $\log_2$ ratio. The thresholds for gain and loss were defined as the $\log_2$ ratio of +0.2 and −0.2, respectively. The BAC clones are all shown contiguously. The underlined BAC clones were used for genome-wide array-CGH. The gray area represents the minimum common region in the 25 cases, which is 500-kb in length between BAC clones RP11–416L21 and RP11–373L24.

Relationship between genomic alteration and expression of *REL* and *BCL11A*

Four of the seven cases analyzed by contig array-CGH showed gain or amplification for both *REL* and *BCL11A* genes, whereas the remaining three demonstrated gain or amplification of *REL* alone (Fig. 4a). To investigate the relationship between genomic amplification and gene expression, we conducted RQ-PCR analysis for both candidate genes in six of the seven cases with 2p15–16 gain whose RNA was available, and in seven cases without any change at 2p15–16 (Fig. 4b). Three cases with copy number gains for both genes (D778, D856 and D1767) demonstrated overexpression for both, and two cases with a copy number gain of *REL* alone (D768 and D1664) showed significant overexpression of *REL*, but the remaining case (D754) showed an expression level beyond the average for normal controls, although the difference was not significant. These three cases showed neither genomic gain nor overexpression of *BCL11A* (D768, D1664 and D754). Correlation coefficients for the $\log_2$ ratio of DNA and the relative amount of mRNA were 0.76 for *REL* and 0.89 for *BCL11A*. These data indicate that overexpression of *REL* and *BCL11A* correlates well with the level of genomic amplification of both genes. Thus, both of these two genes are targets at the 2p15–16 region, whose expression is altered by genomic amplification in DLBCL. Furthermore, we also conducted RQ-PCR in an additional six DLBCL cases with 2p gain, for which contig array-CGH could not be carried out. All of the additional cases except one showed *REL* overexpression in accordance with genomic gain, whereas only four cases showed *BCL11A* overexpression (data not shown).

RT-PCR analysis of the genes within the 2p15–16 amplicon, and RQ-PCR for *LOC344423* and *PEX13*

The contig array-CGH showed that nine genes were located within the 2p15–16 minimum common region (500 kb in length). RT-PCR analysis was used to evaluate expression of these nine genes (Table 1). The cell lines used for screening were B-cell lymphoma cell lines with 2p amplification (RC-K8, L428[28] and Karpas-1106p[29]) and human placenta. The sizes of all products obtained by RT-PCR were confirmed by electrophoresis and were as expected (data not shown). Expression of three genes (*REL*, *LOC344423* and *PEX13*) could be detected in all B-cell lymphoma cell lines with 2p amplification. We conducted RQ-PCR analysis for *LOC344423* and *PEX13* in the same six cases with 2p15–16 gain to investigate the relationship between genomic amplification and gene expression (Fig. 4c,d). All cases but one showed overexpression of *LOC344423* and *PEX13* in a similar fashion to that of *REL*. Correlation coefficients for the $\log_2$ ratio of DNA and the relative amount of mRNA were 0.73 for *LOC344423* and 0.97 for *PEX13*. Thus, both of these genes are also possible targets in the 2p15–16 region in DLBCL, although functional study is needed.

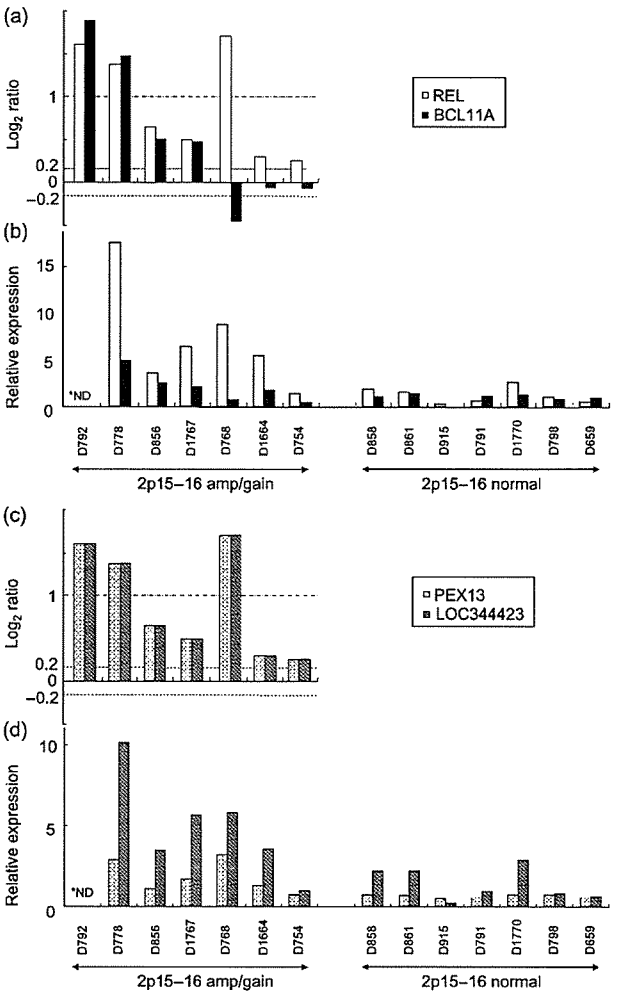

Fig. 4. Relationship between genomic amplification and expression of *REL*, *BCL11A*, *PEX13* and *LOC344423*. (a) Mean $\log_2$ ratio of all bacterial artificial chromosome (BAC) clones containing the *REL* locus and the *BCL11A* locus obtained from contig array-based comparative genomic hybridization (array-CGH). The thresholds for gain and loss were defined as the $\log_2$ ratio of +0.2 and −0.2, respectively. White bars: *REL* locus. Black bars: *BCL11A* locus. (b) Relative expression levels of *REL* and *BCL11A* determined by real-time quantitative-polymerase chain reaction (RQ-PCR) in cases with 2p15–16 gain and those without any change at 2p15–16 (normal). For relative expression levels, each expression was normalized on the basis of the corresponding *G6PDH* content. White bars: *REL*. Black bars: *BCL11A*. *ND: RQ-PCR not done for D792 because RNA was not available. (c) Mean $\log_2$ ratio of all BAC clones containing the *PEX13* locus and the *LOC344423* locus obtained from contig array CGH. The thresholds for gain and loss were defined as the $\log_2$ ratio of +0.2 and −0.2, respectively. Dotted bars: *PEX13* locus. Striped bars: *LOC344423* locus. (d) Relative expression levels of *PEX13* and *LOC344423* detected by RQ-PCR in cases with 2p15–16 gain and of cases without any change at 2p15–16 (normal). For relative expression levels, each expression was normalized on the basis of the corresponding *G6PDH* content. Dotted bars: *PEX13*. Striped bars: *LOC344423*. *ND: RQ-PCR not done for D792 because RNA was not available.

Discussion

Gain of chromosome 2p has been identified as a recurrent alteration in 20% of DLBCL,[9–15] 50% of cHL,[16,17] and 3–47% of PMBCL cases.[11,14,15] In previous studies, CGH and FISH analyses were used as tools to investigate genomic alterations. Array-CGH is superior to these two methods in terms of higher resolution and the ability to directly map the copy number changes to the genome sequence. The genome-wide

doi: 10.1111/j.1349-7006.2006.00209.x

array-CGH with a resolution of 1.3 Mb used for the 99 DLBCL cases enrolled in our study identified a common recurrent 4.5-Mb region at 2p15–16. By carrying out high-resolution contig array-CGH in the recurrent region, we were able to restrict the minimal common region to 500 kb in length.

The *REL* proto-oncogene, which is located in the 2p15–16 region, has been investigated as a target of the region in many reported studies. As *BCL11A* was identified as another oncogene in this region,[30] the two oncogenes have been examined together. In most cHL cases, coamplification of both gene loci was shown by fluorescence immunophenotyping and interphase cytogenetics (FICTION). Bea *et al.* detected simultaneous overexpression of both genes in all DLBCL cases with 2p amplification by means of RQ-PCR.[12]

In the present study, we were able to identify the minimally targeted genomic regions of 2p15–16 amplification where *REL*, not *BCL11A*, is located as the only candidate oncogene. Martin-Subero *et al.* investigated amplification of both gene loci, *REL* and *BCL11A*, in cHL tumors by means of FICTION and reported that one case displayed selective amplification of the *REL* locus and two cases showed signal patterns suggesting breakpoints within the *REL* locus.[16] They concluded that the target of 2p alterations might be closely associated with the *REL* locus, consistent with the region we identified as a minimum common region, although they did not investigate gene expression.

It has been reported that a high copy number of *REL* correlates with extranodal disease in DLBCL.[9] A recent multicenter cooperative study demonstrated that expression of *REL* and *BCL11A* was frequently recognized in the germinal center like B cell (GCB)-DLBCL subgroup that is known to have favorable prognosis. However, the number of cases with 2p gain or amplification in our cohort was too small to draw any definitive conclusions in this respect, but it has been reported that the correlation of 2p gain and favorable outcome could not be demonstrated.[15]

To investigate the correlation between genomic amplification and expression, we carried out RQ-PCR analysis of the candidate genes *REL* and *BCL11A* and found a significant correlation between genomic alteration and expression in both genes. This indicates that both genes are common targets for genomic amplification in this region. However, given the fact that *REL* is more frequently amplified than *BCL11A*, it is speculated that *REL* may play a more important role than *BCL11A* in the development of lymphoma.

Our results identified two additional candidate genes as targets of the 2p15–16 amplicon and demonstrated for the first time the overexpression of *LOC344423 and PEX13* in primary tumors. Because these two genes and *REL* are located within the same BAC (RP11–373L24), it is speculated that the *LOC344423* and *PEX13* loci are also amplified in cases with *REL* locus amplification. However, the coding frame of *LOC344423* is missing nor regulatory RNA, such as micro RNA, is found, and *PEX13* is a structural gene of the peroxisome. This suggests that neither *LOC344423* nor *PEX13* are likely candidate genes for oncogenesis.

Acknowledgments

We are grateful to Dr Yoshitaka Hosokawa, Dr Shinobu Tsuzuki and Dr Ritsuro Suzuki for their discussions and encouragement throughout this study. The outstanding technical assistance of Ms Hiroko Suzuki is very much appreciated. This work was supported in part by Grants-in-Aid from the Ministry of Health, Labor and Welfare, from the Ministry of Education, Culture, Sports Science and Technology, from the Japan Society for the Promotion of Science, and from the Foundation of Promotion of Cancer Research, as well as by a Grant-in-Aid for cancer research from the Princess Takamatsu Cancer Research Fund (03-23503) and the Wella Award from the Japan Leukemia Research Fund awarded to MS.

References

1 The Non-Hodgkin's Lymphoma Classification Project. A clinical evaluation of the International Lymphoma Study Group Classification of non-hodgkin's lymphoma. *Blood* 1997; **89**: 3909–18.
2 Harris NL, Jaffe ES, Stein H *et al.* A revised European–American classification of lymphoid neoplasms: a proposal from the International Lymphoma Study Group. *Blood* 1994; **84**: 1361–92.
3 Offit K, Le Coco F, Louie DC *et al.* Rearrangement of *BCL6* gene as a prognostic marker in diffuse large cell lymphoma. *N Engl J Med* 1994; **331**: 74–80.
4 Kramer MHH, Hermans J, Wijburg E *et al.* Clinical relevance of BCL2, BCL6, and MYC rearrangements in diffuse large B-cell lymphoma. *Blood* 1998; **92**: 3152–62.
5 Gatter KC, Warnke RA. Diffuse large B-cell lymphoma. In Jaffe ES, Harris NL, Stein H, Vardiman JW, eds. *World Health Classification of Tumors. Pathology and Genetics of Tumors of Haematopoietic and Lymphoid Tissues*. Washington: IARC Press, Lyon, 2001; 171–4.
6 Tagawa H, Tsuzuki S, Suzuki R *et al.* Genome-wide array-based comparative genomic hybridization of diffuse large B-cell lymphoma: comparison between CD5-positive and CD5-negative cases. *Cancer Res* 2004; **64**: 5948–55.
7 Tagawa H, Suguro M, Tsuzuki S *et al.* Comparison of genome profiles for identification of distinct subgroups of diffuse large B-cell lymphoma. *Blood* 2005; **106**: 1770–7.
8 Ota A, Tagawa H, Karnan S *et al.* Identification and characterization of a novel gene, *C13orf25*, as a target for 13q31-q32 amplification in malignant lymphoma. *Cancer Res* 2004; **64**: 3087–95.
9 Houldsworth J, Mathew S, Rao PH *et al.* *REL* proto-oncogene is frequently amplified in extranodal diffuse large cell lymphoma. *Blood* 1996; **87**: 25–9.
10 Rao PH, Houldsworth J, Dyomina K *et al.* Chromosomal and gene amplification in diffuse large B-cell lymphoma. *Blood* 1998; **92**: 234–40.
11 Palanisamy N, Abou-Elella AA, Chaganti SR *et al.* Similar patterns of genomic alterations characterize primary mediastinal large B-cell lymphoma and diffuse large B-cell lymphoma. *Genes Chromosomes Cancer* 2002; **33**: 114–22.
12 Bea S, Colomo L, Lopez-Guillermo A *et al.* Clinicopathologic significance and prognostic value of chromosomal imbalances in diffuse large B-cell lymphomas. *J Clin Oncol* 2004; **22**: 3498–506.
13 Houldsworth J, Olshen AB, Cattoretti G *et al.* Relationship between *REL* amplification, REL function, and clinical and biologic features in diffuse large B-cell lymphomas. *Blood* 2004; **103**: 1862–8.
14 Feuerhake F, Kutok JL, Monti S *et al.* NFκB activity, function, and target-gene signatures in primary mediastinal large B-cell lymphoma and diffuse large B-cell lymphoma subtypes. *Blood* 2005; **106**: 1392–9.
15 Bea S, Zettl A, Wright G *et al.* Diffuse large B-cell lymphoma subgroups have distinct genetic profiles that influence tumor biology and improve gene expression-based survival prediction. *Blood* 2005; **106**: 3183–90.
16 Martin-Subero JI, Gesk S, Harder L *et al.* Recurrent involvement of the *REL* and *BCL11A* loci in classical Hodgkin lymphoma. *Blood* 2002; **99**: 1474–7.
17 Joos S, Menz CK, Wrobel G *et al.* Classical Hodgkin lymphoma is characterized by recurrent copy number gains of the short arm of chromosome 2. *Blood* 2002; **99**: 1381–7.

18 Goff LK, Neal MJ, Crawley CR *et al.* The use of real-time quantitative polymerase chain reaction and comparative genomic hybridization to identify amplification of the *REL* gene in follicular lymphoma. *Br J Haematol* 2000; **111**: 618–25.
19 Pinkel D, Segraves R, Sudar D *et al.* High resolution analysis of DNA copy number variation using comparative genomic hybridization to microarrays. *Nat Genet* 1998; **20**: 207–11.
20 Telenius H, Carter NP, Bebb CE *et al.* Degenerate oligonucleotide-primed PCR: general amplification of target DNA by a single degenerate primer. *Genomics* 1992; **13**: 718–25.
21 Kameoka Y, Tagawa H, Tsuzuki S *et al.* Contig array CGH at 3p14.2 points to the *FRA3B/FHIT* common fragile region as the target gene in diffuse large B cell lymphoma. *Oncogene* 2004; **23**: 9148–54.
22 Kasugai Y, Tagawa H, Kameoka Y, Morishima Y, Nakamura S, Seto M. Identification of *CCND3* and *BYSL* as candidate targets for 6p21 amplification in diffuse large B-cell lymphoma. *Clin Cancer Res* 2005; **11**: 8265–72.
23 Kubonishi I, Niiya K, Miyoshi I. Establishment of a new human lymphoma line that secretes plasminogen activator. *Jpn J Cancer Res* 1985; **76**: 12–15.
24 Schaadt M, Fonatsch C, Kirchner H, Diehl V. Establishment of a malignant, Epstein–Barr virus (EBV)-negative cell-line from the pleura effusion of a patient with Hodgkin's disease. *Blut* 1979; **38**: 185–90.
25 Nacheva E, Dyer MJ, Metivier C *et al.* B-cell non-Hodgkin's lymphoma cell line (Karpas 1106) with complex translocation involving 18q21.3 but lacking *BCL2* rearrangement and expression. *Blood* 1994; **84**: 3422–8.
26 Takizawa J, Suzuki R, Kuroda H *et al.* Expression of the *TCL1* gene at 14q32 in B-cell malignancies but not in adult T-cell leukemia. *Jpn J Cancer Res* 1998; **89**: 712–18.
27 Suguro-Katayama M, Suzuki R, Kasugai Y *et al.* Heterogeneous copy numbers of API2-MALT1 chimeric transcripts in mucosa-associated lymphoid tissue lymphoma. *Leukemia* 2003; **17**: 2508–12.
28 Joos S, Granzow M, Holtgreve-Grez H *et al.* Hodgkin's lymphoma cell lines are characterized by frequent aberrations on chromosomes 2p and 9p including *REL* and *JAK2*. *Int J Cancer* 2003; **103**: 489–95.
29 Joos S, Otano-Joos MI, Ziegler S *et al.* Primary mediastinal (thymic) B-cell lymphoma is characterized by gains of chromosomal material including 9p and amplification of the *REL* gene. *Blood* 1996; **87**: 1571–8.
30 Satterwhite E, Sonoki T, Willis TG *et al.* The *BCL11* gene family: involvement of *BCL11A* in lymphoid malignancies. *Blood* 2001; **98**: 3413–20.

doi: 10.1111/j.1349-7006.2006.00209.x

Randomized phase II study of concurrent and sequential rituximab and CHOP chemotherapy in untreated indolent B-cell lymphoma

Michinori Ogura,[1,9] Yasuo Morishima,[1] Yoshitoyo Kagami,[1] Takashi Watanabe,[2] Kuniaki Itoh,[3] Tadahiko Igarashi,[3] Tomomitsu Hotta,[4] Tomohiro Kinoshita,[5] Yasuo Ohashi,[6] Shigeo Mori,[7] Takashi Terauchi[8] and Kensei Tobinai[2]

[1]Department of Hematology and Cell Therapy, Aichi Cancer Center, 1-1 Kanokoden, Chikusa-ku, Nagoya 464-8681; [2]Hematology and Stem Cell Transplantation Division, National Cancer Center Hospital, 5-1-1 Tsukiji, Chuo-ku, Tokyo 104-0045; [3]Hematology and Oncology Division, National Cancer Center Hospital East, 6-5-1 Kashiwanoha, Kashiwa, Chiba 277-8577; [4]Department of Hematology and Oncology, Tokai University School of Medicine, Bohseidai, Isehara, Kanagawa 259-1193; [5]First Department of Internal Medicine, Nagoya University School of Medicine, Nagoya 466-8560; [6]Biostatistics Sciences, School of Health Science and Nursing Biostatistics, University of Tokyo, 7-3-1 Hongo, Bunkyo-ku, Tokyo 113-8655; [7]Department of Pathology, Institute of Medical Science, University of Tokyo, Shirokanedai, Minato-ku, Tokyo 108-8639; and [8]Research Center for Cancer Prevention and Screening, National Cancer Center, 5-1-1 Tsukiji, Chuo-ku, Tokyo 104-0045, Japan

(Received October 16, 2005/Revised December 26, 2005/Accepted December 26, 2005/Online publication March 30, 2006)

CHOP combined with rituximab (R-CHOP) is regarded as one of the most effective treatments for indolent B-cell non-Hodgkin lymphoma (B-NHL), however, its optimal combination schedule remains unknown. We performed a randomized phase II study to explore a more promising schedule in untreated, advanced indolent B-NHL. Patients were randomized to receive either six courses of CHOP concurrently with rituximab (Arm C), or six courses of CHOP followed by six courses of weekly rituximab (Arm S). A total of 69 patients received the concurrent (n = 34) or sequential (n = 35) regimen. Overall response rate (ORR) in Arm C was 94% (95% confidence interval [CI], 79 to 99), including a 66% complete response (CR) compared with 97% (95% CI, 85–100), including a 68% CR in Arm S. Patients in Arm C experienced more grade 4 neutropenia (85% *versus* 70%) and experienced more grade 3 or greater non-hematological toxicities (21% *versus* 12%). Both arms were tolerated well. With a median follow-up of 28.2 months, the median progression-free survival (PFS) time was 34.2 months in Arm C, and was not reached in Arm S. R-CHOP is highly effective in untreated indolent B-NHL, either concurrent or in a sequential combination. Both combination schedules deserve further investigation. (*Cancer Sci* 2006; 97: 305–312)

Indolent non-Hodgkin lymphomas (NHLs), in which the representative type of lymphoma is follicular lymphoma (FL), are characterized by an advanced stage at presentation, lack of symptoms associated with the disease, and indolent behavior in terms of the time to symptomatic disease progression.[1,2] Although many chemotherapeutic agents and combination therapies are used in the treatment of patients with FL, a large majority of these patients remain incurable.[3–5] Thus, more effective strategies are needed to overcome the current therapeutic limitations. Rituximab is a chimeric monoclonal anti-CD20 antibody that can deplete malignant B cells through complement-dependent cytotoxicity, antibody-dependent cell-mediated cytotoxicity (ADCC),[6] and apoptotic mechanisms.[7] It has also been shown to sensitize lymphoma cell lines resistant to cytotoxic drugs.[8] In recent years, it was demonstrated that rituximab is an active agent against indolent B-NHL and has become a standard component of first-line therapy, either as a single agent or in combination with chemotherapy.[9–18] Recently, the addition of rituximab to the cyclophosphamide, doxorubicin, vincristine and prednisolone (CHOP) regimen or cyclophosphamide, vincristine and prednisolone (CVP) regimen was demonstrated to improve the clinical outcome in patients with previously untreated advanced FL, without increased toxicity. Czuczman *et al.* conducted the first phase II study on the combination of rituximab with CHOP in mostly untreated patients with low-grade B-NHL or FL.[14] They treated the patients with six cycles of standard CHOP given at 3-week intervals along with rituximab administered twice before, during and after the six cycles of CHOP therapy. All treated patients (n = 38) responded with a complete response (CR) rate of 87%, and the median time to progression (TTP) was 82.3 months.[15] Marcus *et al.* reported significant superiority of CVP plus rituximab (R-CVP) over CVP for previously untreated patients with advanced FL in a randomized phase III study.[18] From the viewpoint of the possible synergistic effect between rituximab and chemotherapeutic drugs, it seems to be reasonable that rituximab be delivered in combination with chemotherapeutic drugs concurrently. Whereas, from the viewpoint of enhancing the ADCC effect, which is one of the putative antitumor mechanisms of rituximab, it seems reasonable that rituximab be administered in situations in which effector cells such as macrophages, natural killer cells and neutrophils are intact, in other words, there are no cytotoxic or immunosuppressive effects of chemotherapeutic drugs. Thus, to maximize the

[9]To whom correspondence should be addressed. E-mail: mi-ogura@naa.att.ne.jp
Present address: The Department of Hematology, Nagoya Daini Red Cross Hospital, 2-9, Myokencho, Showaku, Nagoya 466-8650, Japan.
Portions of this study were presented at the Annual Meeting of the American Society of Clinical Oncology, New Orleans, 2004.

doi: 10.1111/j.1349-7006.2006.00173.x

possible ADCC effect, it might be preferable that rituximab be delivered to patients after recovery from the toxic or immunosuppressive effect of chemotherapy. However, the optimal schedule for the combined use of rituximab and chemotherapy remains unclear. To explore a more promising regimen of rituximab combined with CHOP therapy for the treatment of indolent B-cell NHL, we conducted a randomized phase II trial.

Materials and Methods

Patients

Between July 1999 and July 2000, 69 patients with newly diagnosed indolent B-cell NHLs were enrolled. Eligibility criteria included: aged between 20 and 70 years; a histopathological diagnosis of indolent B-NHL according to the Revised European-American Lymphoma (REAL) classification[19] (including small lymphocytic lymphoma, lymphoplasmacytic lymphoma, FL or marginal zone B-cell lymphoma); no previous treatment; stages III or IV disease according to the Ann Arbor staging system;[20] CD20 positive lymphomas confirmed by immunohistochemistry or flow cytometry; an Eastern Cooperative Oncology Group (ECOG)[21] performance status (PS) of 0, 1 or 2; negative for the hepatitis B virus surface antigen, hepatitis C virus antibody or human immunodeficiency virus antibody; having no other malignancies and normal renal, pulmonary and hepatic function. Approval was obtained from the local institutional review boards of all participating institutions. Informed consent was obtained from all patients before enrollment in accordance with the Declaration of Helsinki.

Study design

This randomized phase II study was designed as a two arm parallel phase II study. The expected overall response rate (ORR) (P1) for either arm was set at 95% based on the phase II study by Czuczman *et al.* where CHOP was combined with rituximab,[14] while the threshold response rate (P0) was set at 75%, based on previous reports on CVP or COP, CHOP or CHOP-like studies.[22] The number of patients required for this study was 27 per arm, calculated in accordance with Fleming's two-stage testing procedure,[23] at $\alpha = 0.05$ (two-side) and $1\text{-}\beta = 0.8$. Assuming that up to 20% of patients might be ineligible due to inaccurate histopathological diagnosis at participating institutions, we planned to enroll at least 34 patients per arm. From the viewpoint of selection design by Simon *et al.*,[24] the selection of one arm showing a 15% higher percentage CR at 90% probability would be possible with this number of patients, if the percentage CR of both arms would achieve at least 65%.

Treatment schedule

Patients fulfilling the inclusion criteria were randomly assigned to either the concurrent arm (Arm C) or sequential arm (Arm S) at the independent randomization center, thereby minimizing the bias between the arms regarding PS, clinical stage and institution. All patients were treated with six courses of standard CHOP chemotherapy (cyclophosphamide 750 mg/m^2, i.v., day 1; doxorubicin 50 mg/m^2 i.v., day 1; vincristine 1.4 mg/m^2 [capped at 2 mg] i.v., day 1; and prednisolone 100 mg, p.o., days 1–5) every 3 weeks. In addition, patients allocated to Arm C received rituximab (375 mg/m^2 i.v.) 2 days prior to each CHOP cycle, whereas patients allocated to Arm S received rituximab (375 mg/m^2, weekly six times, i.v.) 4 weeks after completion of the sixth cycle of CHOP. Rituximab was given intravenously based on the preceding phase I study in Japan.[25]

Patient evaluation, end-points and response criteria

Patients were observed until the progression of lymphomas or death. Tumor restaging was performed at approximately 3-monthly intervals for the first 12 months and every 4 to 6 months thereafter.

The primary end-point of this study was an ORR in all eligible patients, that is, the percentage of patients achieving a CR, CRu, or partial response (PR), evaluated according to the International Workshop Response Criteria for NHL.[26] CR required the disappearance of all detectable clinical and radiographic evidence of disease, disappearance of disease-related symptoms, and normalization of biochemical abnormalities. Adenopathy on computed tomography (CT) scans must have regressed to normal size (1.5 cm or less in the greatest transverse diameter). CRu was defined as complete disappearance of all detectable clinical and radiographic abnormalities of the disease, with the exception of the presence of a residual adenopathy larger than 1.5 cm, as long as the sum of products of the greatest diameters (SPDs) of the adenopathy had decreased by more than 75%. Residual bone marrow abnormalities, that included increased number or size of lymphoid aggregates without definite cytological evidence of persistent lymphoma, could also be present in patients in the CRu response category. PR was defined as a greater than 50% decrease in the SPDs of the largest dominant nodes or nodal masses. Stable disease patients were defined as having any response that was less than a PR or an increase in the SPDs by less than 25%, with no new lesions appearing. Progressive disease was defined by an increase of more than 25% in the size of the SPDs of the measured lesions, or the appearance of new lesions. All cases were centrally reviewed radiographically using CT films.

Secondary end-points were percentage CR, including percentage CRu and a progression-free survival (PFS) for all eligible patients, as an interval from the day of enrollment to the first day when tumor progression or death due to any cause was observed. The response to the combined regimen and PFS period for each patient was evaluated until at least 2 and a half years after the completion of treatment.

Adverse events (AEs) were graded according to the toxicity criteria of the Japan Clinical Oncology Group,[27] an expanded version of the Common Toxicity Criteria of the National Cancer Institute (version 1.0).

Human antichimeric antibody assay and pharmacokinetics of rituximab

Serum human antichimeric antibody (HACA) levels were monitored at 8 and 10 months after treatment initiation using an enzyme-linked immunosorbent assay (ELISA), as described previously.[28]

Serum rituximab levels were monitored using ELISA for patients who signed another informed consent form to participate in this pharmacokinetic (PK) study. The PK parameters were calculated using WinNonlin PK software (WinNonlin

doi: 10.1111/j.1349-7006.2006.00173.x

Standard Japanese Edition, version 1.1; Scientific Consulting, Apex, NC, USA).

Statistical methods

The ORR, percentage CR, and their 95% confidence intervals (CIs) were calculated with per protocol sets (PPS) of data for all eligible patients and full analysis sets (FAS) of data for all enrolled patients under the F-distribution. The median PFS time, time to CR (TTCR) and time to response (TTR), and their 95% CIs were estimated for all eligible and evaluative patients using the method of Kaplan and Meier, and were compared using the log–rank test. In addition, pretreatment factors affecting the ORR and PFS were analyzed for all eligible and evaluative patients by univariate and multivariate analyses using Fisher's exact test, Wilcoxon's rank sum test, the log–rank test, the logistic regression model or Cox's proportional hazard regression model.

All statistical analyses were performed using SAS software (version 6.12; SAS Institute, Cary, NC, USA). Data used for theses analyses were finally confirmed on March 31, 2004.

Results

Patient characteristics

A total of 69 patients were enrolled from 21 institutions (see Appendix I); 34 patients were allocated to Arm C and 35 patients to Arm S. Patient characteristics at study entry are summarized in Table 1. The median age was 52 years (range, 26–69 years). The major characteristics of the two arms were very similar in both the enrolled and eligible patients. Retrospectively, we analyzed the Follicular Lymphoma International Prognostic Index (FLIPI) in all patients.[29] FLIPI was equally distributed between the two arms. Twenty-eight patients (82%) in Arm C and 30 patients (86%) in Arm S were judged

Table 1. Patient characteristics

Factor	Enrolled (n = 69)			Eligible (n = 66)		
	Arm C	Arm S	Total	Arm C	Arm S	Total
Sex						
Female	18	18	36	17	18	35
Male	16	17	33	15	16	31
Age (years)						
Median	53	50	52	54.5	49.5	52.5
Range	36–65	26–69	26–69	36–65	26–69	26–69
Performance status (ECOG)						
0	29	30	59	28	29	57
1	5	5	10	4	5	9
Histopathology (REAL)†						
Follicular, grade 1	12	11	23	11	11	22
Follicular, grade 2	21	19	40	20	19	39
Follicular, grade 3	0	2	2	0	2	2
Marginal zone B-cell	1	0	1	1	0	1
Low grade B-NHL, NOS‡	0	2	2	0	2	2
No specimen submitted§	0	1	1	0	0	0
Clinical stage (Ann Arbor)						
III	14	15	29	13	14	27
IV	20	20	40	19	20	39
B-symptoms						
Absent	30	33	63	29	32	61
Present	4	2	6	3	2	5
LDH						
Normal	32	31	63	31	30	61
Elevated	2	4	6	1	4	5
No. of extranodal sites						
0–1	25	26	51	24	25	49
≤2	9	9	18	8	9	17
International Prognostic Index						
Low	21	21	42	21	20	41
Low-intermediate	12	12	24	10	12	22
High-intermediate	1	1	2	1	1	2
High	0	1	1	0	1	1
Follicular Lymphoma International Prognostic Index						
Low	16	15	31	16	15	31
Intermediate	12	15	27	10	14	25
High	6	5	11	5	5	10

†According to the diagnosis by the central pathology review. ‡Low-grade B-cell non-Hodgkin lymphoma (NHL) not otherwise specified. §Specimen was not submitted to the central pathology review. LDH, lactic dehydrogenase.

Table 2. Response to therapy

Arm		n	No. of patients achieving response						Response rate (95% CI)	
			CR	CRu	PR	SD	PD	NE	%CR	ORR
Arm C	Eligible	32	19 21 30	2	9	1	0	1	66% (47–81%)	94% (79–99%)
	Enrolled	34	21 23 33	2	10	1	0	0	68% (50–83%)	97% (85–100%)
Arm S	Eligible	34	22 23 33	1	10	0	0	1	68% (50–83%)	97% (85–100%)
	Enrolled	35	21 23 33	1	10	0	0	2	66% (44–81%)	94% (81–99%)

Response to each therapy was evaluated according to the International Workshop Criteria for Non-Hodgkin's Lymphoma. CI, confidence interval; CR, complete response; CRu, complete response/unconfirmed; NE, not evaluative due to insufficient follow-up; ORR, overall response rate; PD, progressive disease; PR, partial response; SD, stable disease.

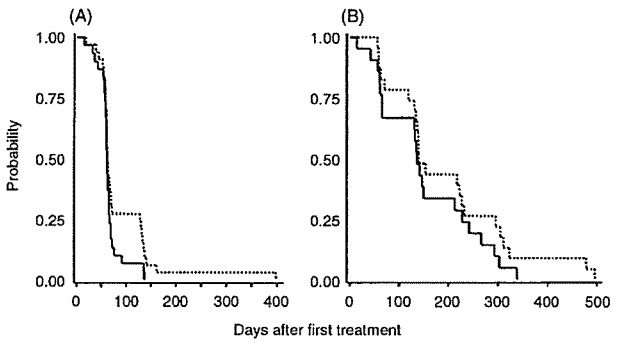

Fig. 1. (A) Time to response (TTR) and (B) time to complete response (TTCR). Medians were estimated by the Kaplan-Meier method. A total of 63 patients (Arm C [-], 30; Arm S [---], 33) were analyzed for TTR, and 44 patients (Arm C, 21; Arm S, 23) for TTCR with per protocol sets of data. Median TTRs in Arm C and Arm S were 61 days (95% confidence interval [CI] 59 to 65 days) and 62 days (95% CI 60–70 days), respectively. The 75th percentile TTRs in Arm C and Arm S were 66 days (95% CI 63 to 76 days) and 140 days (95% CI 66–135 days), respectively ($P = 0.0994$, log–rank test). Median TTCRs in Arm C and Arm S were 136 days (95% CI 65 to 213 days) and 140 days (95% CI 134–227 days), respectively. The 75th percentile TTCRs in Arm C and Arm S were 228 days (95% CI 141 to 293 days) and 295 days (95% CI 153–323 days), respectively ($P = 0.2201$, log–rank test).

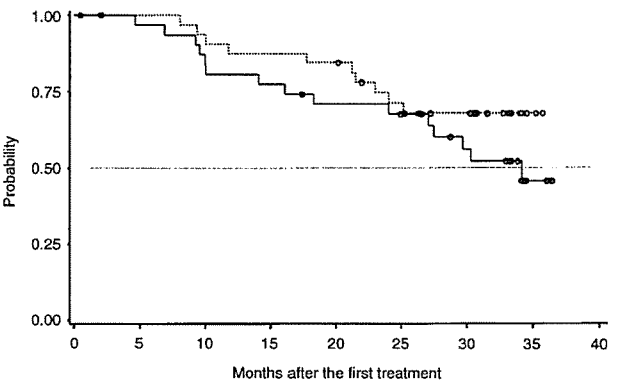

Fig. 2. Progression-free survival (PFS). Medians were estimated by the Kaplan-Meier method. The upper limit of the 95% confidence interval (CI) for Arm C has not yet been determined. A total of 65 patients (Arm C, 32; Arm S, 33) were analyzed with per protocol sets of data. The median PFS time for patients in Arm C (-) was 34.2 months (95%CI, 27.1 months, inestimable), whereas that for patients in Arm S (...) had not yet been reached, with a median follow-up time of 28.2 months. Log–rank test, $P = 0.220$. (o) Censored.

to belong to the low, or low-intermediate risk group categorized by FLIPI. Three patients were judged ineligible by an extramural review committee, because two of them had concomitant active cancer and one had a history of prior chemotherapy, including doxorubicin for the treatment of breast cancer. Sixty-five patients (94%) were confirmed to have FL in the central pathology review.

Response to treatment and survival

Sixty-six eligible patients (Arm C, 32 patients; Arm S, 34 patients) were evaluated with PPSs of data, and 69 patients (Arm C, 34 patients; Arm S, 35 patients) with FASs of data. One patient allocated to Arm C could not be evaluated for response because the first cycle of chemotherapy given was not CHOP (doxorubicin in the CHOP regimen was erroneously replaced with daunorubicin). Two patients (one patient eligible and one ineligible) allocated to Arm S could not be evaluated because they had withdrawn from the study before starting treatment.

As shown in Table 2, similar results of the ORRs and the percentage CRs were obtained in Arm C and Arm S. The ORRs and percentage CRs calculated with PPSs and FASs were similar. Kaplan-Meier curves of TTR and TTCR were plotted for eligible and evaluative patients in each arm, as shown in Fig. 1. Although the median TTRs for patients in Arm C and Arm S were not different (61 days *versus* 62 days, respectively), the 75th percentile TTRs for patients were shorter in Arm C (66 days) than Arm S (127 days), with no statistical difference ($P = 0.0994$, log–rank test). The median TTCRs were similar in Arm C and Arm S (136 days and 140 days, respectively). As shown in Fig. 2, the median PFS time for patients in Arm C ($n = 32$) was 34.2 months

doi: 10.1111/j.1349-7006.2006.00173.x

Table 3. Hematological toxicity

Toxicity	Arm	*n*	Grade 0–2	Grade 3	Grade 4
Any hematological toxicity	Arm C	34	2 (6%)	3 (9%) 32 (94%)	29 (85%)
	Arm S	33	0 (0%)	10 (30%) 33 (100%)	23 (70%)
Leukopenia	Arm C	34	5 (15%)	16 (47%) 29 (85%)	13 (38%)
	Arm S	33	3 (9%)	23 (70%) 30 (91%)	7 (21%)
Neutropenia	Arm C	34	2 (6%)	3 (9%) 32 (94%)	29 (85%)
	Arm S	33	1 (3%)	9 (27%) 32 (97%)	23 (70%)
Thrombocytopenia	Arm C	34	32 (94%)	1 (3%) 2 (6%)	1 (3%)
	Arm S	33	33 (100%)	0 (0%) 0 (0%)	0 (0%)
Anemia	Arm C	34	31 (91%)	3 (9%)	–
	Arm S	33	31 (94%)	2 (6%)	–

Hematological toxicity was evaluated according to the JCOG Toxicity Criteria, an expanded version of the NCI-CTC version 1.0. All hematological toxicities (possibly related to rituximab, or unknown relationship to rituximab) observed during the treatment and follow-up period (for 6 months after the last cycle of CHOP for Arm C, and for 4 months after the last rituximab infusion for Arm S) are listed.

(95%CI, 27.1 months – inestimable), whereas that for patients in Arm S ($n = 33$) had not yet been reached, with a median follow-up time of 28.2 months. One patient (#38) in Arm S died of tumor progression 730 days after the first treatment. No other patients died within approximately 3 years of observation.

Adverse events

Information about AEs was available for 67 patients (Arm C, 34 patients; Arm S, 33 patients) who received protocol treatment. Hematological toxicity was documented at its highest grade throughout the study period. As shown in Table 3, major hematological toxicity was neutropenia; grade 3 or greater neutropenia was observed in 32 patients (94%) in Arm C and in 33 patients (100%) in Arm S; grade 4 neutropenia was seen in 29 patients (85%) in Arm C and in 23 patients (70%) in Arm S. All hematological toxicities were controllable and reversible, although some patients required hematopoietic cytokines.

Grade 3 or greater non-hematological AEs observed during treatment and initial follow-up periods are listed in Table 4. A total of 11 patients (Arm C, seven patients, 21%; Arm S, four patients, 12%) developed 14 events of grade 3 or greater non-hematological adverse events. All non-hematological toxicities were reversible. There was no therapy-related death.

Prognostic factors

Pretreatment factors affecting ORR and PFS were analyzed. Because the sample size of each arm was small, analyses were not performed separately for the two arms, but results were pooled ($n = 64$). There were two factors affecting ORR when analyzed by the Wilcoxon's rank sum test. Patients with PS 0 (41CR, 13PR, 1NC, 0 PD) demonstrated a superior response to those with PS 1 (3CR, 6PR, 0NC, 0PD) ($P = 0.0182$, Wilcoxon's rank-sum). Patients with a tumor size <5 cm (32CR, 6PR, 1NC, 0 PD) had a superior response to those with tumors equal to 5 cm (12CR, 13PR, 0NC, 0 PD) ($P = 0.0066$, Wilcoxon's rank-sum).

However, no factor significantly affected PFS. Multivariate analyses were also performed using the same factors, excluding IPI. There was no factor that independently affected ORR and PFS.

HACA and pharmacokinetics of rituximab

Out of 67 patients who received rituximab, HACA assays were performed for 65 patients (Arm C, 33; Arm S, 32) at 8 months after treatment, and for 64 patients (Arm C, 33; Arm S, 31) at 10 months after treatment. No patient developed HACA. For all 27 patients (Arm C, 14; Arm S 13) who received four rituximab infusions and whose planned monitoring of

Table 4. Grade 3 or greater-non-hematological adverse events

Arm	Patient	Serious adverse event†	Grade‡	Onset timing	Relating drug (causative)
Arm C	#04	Hyperglycemia	3	6th cycle (day 4)	CHOP (diabetes)
(*n* = 32)	#07	Hyperglycemia	3	4th cycle (day 2)	CHOP, rituximab
	#13	Hypertension	3	1st cycle (day 3)	CHOP, rituximab
	#21	Total bilirubin elevation	3	2nd cycle (day 5)	– (constitutional)
	#23	Abdominal pain	3	1st cycle (day 9)	CHOP, rituximab
	#58	Acute cholangitis with elevated AST and ALT	3	3rd cycle (day 10)	CHOP, rituximab
	#59	Hyperglycemia, hypertension	3	5th cycle (day 6)	CHOP, rituximab
Arm S	#25	Total bilirubin elevation	3	6th cycle (day 132)	– (constitutional)
(*n* = 33)	#56	Diarrhea	4	1st cycle (day 13)	– (alimentary)
		Febrile neutropenia	3	3rd cycle (day 12)	CHOP
		Interstitial pneumonia	3	3rd cycle (day 15)	CHOP
	#62	Total bilirubin elevation	3	4th cycle (day 7)	CHOP
	#69	AST and ALT elevation	3	1st cycle (day 10)	CHOP
				2nd cycle (day 8)	CHOP
				6th cycle (day 29)	CHOP

†Grade 3 or greater adverse events other than hematological toxicities that were observed during the treatment and follow-up period (for 6 months after the last cycle of CHOP for Arm C, and for 4 months after the last rituximab infusion for Arm S). ‡JCOG Toxicity Criteria, an expanded version of the NCI-CTC, version 1.0.

Table 5. Pharmacokinetic parameters of rituximab

Arm		Dose (mg/day)	AUC (μg. h/mL)	Cmax[†] (μg/mL)	$T_{1/2}$ (h)	Clearance[‡] (litter/h)	MRT (h)	Vd (litter)
Arm C	Mean	593.9	372 498.9	262.5	232.3	0.0259	335.1	4.49
(n = 14)	SD	51.1	111 660.4	73.2	113.8	0.0301	164.2	0.66
Arm S	Mean	596.4	418 901.3	433.5	356.9	0.0128	514.9	5.57
(n = 13)	SD	82.6	107 002.6	134.9	163.4	0.0077	235.9	1.95

[†]Actual measured value. [‡]Calculated under the one-compartment model. Time points for serum collection were as follows; Arm C: before, and 10 min and 2 days after each rituximab infusion, and 1 week, 1, 4 and 6 months after the sixth rituximab infusion. Arm S: before, 10 min after each rituximab infusion and 2 days, 1 and 2 weeks, and 1 and 4 months after the sixth rituximab infusion. AUC, area under the curve; Cmax, maximum concentration; $T_{1/2}$, elimination half-life; MRT, mean residence time; Vd, volume of distribution.

serum rituximab levels were completed, pharmacokinetic parameters were calculated throughout the four infusions. As shown in Table 5, Arm S showed higher values for the parameters of area under the curve (AUC), maximum concentration (Cmax), elimination half-life (T1/2), mean residence time (MRT), and volume of distribution (Vd).

Discussion

In this randomized phase II trial, we have demonstrated that the combined use of rituximab and CHOP yielded an ORR of 94% and 97%, and a percentage CR of 66% and 68% in the concurrent arm and the sequential arm, respectively. These ORRs and percentage CRs are superior to those reported for combination chemotherapy regimens containing anthracycline without rituximab, which were conducted after stringent clinical staging with CT. The percentage CR obtained by six to eight cycles of CHOP chemotherapy in untreated patients (n = 83) with FL was reported to be 36% (90%CI, 27–46%).[30] The ORR and percentage CR of CHOP chemotherapy obtained by Kimby *et al.* in their randomized study comparing chlorambucil plus prednisone *versus* CHOP in symptomatic low-grade NHL (n = 127), were 60% and 18%, respectively.[31]

Data of the present study was comparable to the preceding study on CHOP combined with rituximab in patients with indolent B-NHL regarding efficacy and tolerability. Although the precise schedule of the administration of rituximab in the first phase II study of R-CHOP reported by Czuczman *et al.* was not the same as that of the present study, the concept of concurrent use is identical between their trial and Arm C in the present study.[14] However, the percentage CR of Arm C is less than that of Czuczman *et al.*'s trial, and the median PFS of Arm C appears to be shorter in the present study, although more than 82% of all enrolled patients in our study were in the low or low-intermediate risk group by FLIPI. In Czuczman *et al.*'s trial, as the last two infusions of rituximab were administered 1 month after the sixth CHOP cycle, like in our sequential arm, the design of Czuczman *et al.*'s trial had characteristics of both the concurrent arm and the sequential arm. So it is possible that the higher percentage CR and longer PFS in Czuczman *et al.*'s trial compared to our concurrent arm were partly due to the mixed design of the administration schedule of rituximab, in addition to the possible selection bias in phase II studies.

The South-west Oncology Group (SWOG) in the USA studied six cycles of CHOP followed by four weekly infusions of rituximab in newly diagnosed patients with FL at advanced stages (31% with bulky disease and 30% with B-symptoms). Sixteen (19%) of the 84 evaluative patients had an improved tumor response after rituximab treatment, with an ORR of 72%, including 54% with a CR or CRu. The PFS was 76% at the median follow-up of 2.7 years.[32] The PFS data of the sequential arm in our trial is similar to that of the SWOG trial.

Cancer and Leukemia Group B (CALGB) conducted a randomized phase II study to explore a more suitable administration schedule of rituximab with fludarabine in previously untreated chronic lymphocytic leukemia (CLL) patients.[33] Patients randomly received either six monthly courses of fludarabine concurrently with rituximab followed 2 months later by four weekly doses of rituximab for consolidation therapy, or fludarabine alone followed 2 months later by rituximab consolidation therapy. The ORR with the concurrent regimen was 90% compared to 77% with the sequential regimen. With a median follow-up time of 23 months, the number of relapsed patients was 18 (35%) in the concurrent regimen and 15 (28%) in the sequential regimen. Although PFS and survival appeared to be somewhat longer with the sequential treatment, CALGB concluded that the concurrent use of rituximab and fludarabine was superior. Our randomized phase II study for indolent B-cell NHLs showed similar percentage ORRs and percentage CRs between the two arms, and a seemingly longer PFS in the sequential arm. Because patients in the concurrent arm in the CALGB study received consolidated administration of rituximab after induction therapy, the concurrent arm in the CALGB study had characteristics of the concurrent arm and sequential arm of our present study.

In a randomized phase III study that compared eight cycles of R-CVP to CVP for previously untreated patients with advanced FL, a significantly prolonged TTP of R-CVP was reported (median 32 months *versus* 15 months for CVP; $P < 0.0001$).[18] The median TTP of R-CVP was similar to the median PFS of Arm C in our study. As the toxicity is stronger in CHOP than CVP, it is worthwhile to conduct a randomized phase III trial to compare R-CHOP to R-CVP.

The maintenance use of rituximab after first-line rituximab therapy was also reported to prolong PFS or event-free survival (EFS).[34,35] Future trials to explore the role of maintenance use of rituximab after first-line rituximab containing chemotherapy like Arm C are warranted.

About 25% of patients in Arm S did not achieve a response (PR or higher) before the initiation of rituximab treatment, despite the completion of six cycles of CHOP. In Arm C, more than 90% of patients showed a response after the six cycles of CHOP plus rituximab. The same tendency was also shown in the TTCR, as shown in Fig. 1B. The TTCR of each patient in Arm C was relatively shorter than that in Arm S.

doi: 10.1111/j.1349-7006.2006.00173.x

While grade 3 or greater non-hematological AEs were observed in 11 patients (Arm C, seven patients, 21%; Arm S, four patients, 13%), both arms were well tolerated. Two patients were withdrawn from the study before completion of the planned treatment by AE. One patient in Arm C developed acute cholangitis after the third cycle of CHOP plus rituximab. The other patient in Arm S developed interstitial pneumonia after the third cycle of CHOP. Both patients fully recovered. Hematological toxicities were observed in all treated patients; grade 4 neutropenia was frequent and was observed in 85% of patients in Arm C and in 70% in Arm S. However, these hematological toxicities were manageable with or without supportive care using hematopoietic growth factor. No patient was withdrawn from the study due to hematological toxicity. Grade 3 or greater thrombocytopenia was rare in Arm C and absent in Arm S. Although hematological and non-hematological toxicities were slightly more frequent in Arm C, toxicities were clinically acceptable in both arms.

In conclusion, CHOP combined with rituximab was highly effective in untreated patients with indolent B-NHL, especially FL, either in a concurrent or sequential combination, with acceptable toxicities. Although the time to achieve a response was more rapid with the concurrent combination than the sequential combination, PFS appeared to be slightly longer with the sequential combination, although the difference was not statistically significant. We conclude that both combination schedules deserve further investigation. Considering the promising results of rituximab maintenance therapy reported by other investigators, it would be worthwhile to conduct future trials to establish the role of rituximab maintenance after concurrent and sequential combinations of rituximab plus CHOP therapy.

Acknowledgments

This study was supported by Zenyaku Kogyo, Tokyo, Japan. We thank all the investigators, including the physicians, nurses and laboratory technicians, in the participating institutions of this multicenter trial. We are grateful to Dr K. Oshimi (Juntendo University School of Medicine, Tokyo), Dr K. Toyama (Tokyo Medical College, Tokyo), and Dr S. Shirakawa (Koudoukai Hospital, Osaka) for their critical review of the clinical data as members of the Independent Monitoring Committee. We are grateful to Dr S. Nakamura (Aichi Cancer Center Hospital, Nagoya), Dr Y. Matsuno (National Cancer Center Hospital, Tokyo), Dr S. Nawano (National Cancer Center Hospital East, Kashiwa), and Dr M. Matsusako (St. Luke's International Hospital, Tokyo) for their central pathological or radiographical review as members of the Central Pathological Review Committee and the Central Response-Evaluating Committee. We also acknowledge Y. Arita, K. Endo, T. Uesugi, M. Tachikawa, Y. Ikematsu, T. Itoh, H. Iimura, K. Inatomi, M. Ikenami, Y. Koide and T. Kayo (Zenyaku Kogyo) for their help with data collection and statistical and pharmacological analyses.

References

1 Rohatiner A, Lister TA. *Follicular lymphoma, in Magrath IT (ed.): The Non-Hodgkin's Lymphomas*. London: Oxford University Press, 1997: 867–96.
2 Berger F, Felman P, Sonet A *et al.* Nonfollicular small B-cell lymphomas: a heterogeneous group of patients with distinct clinical features and outcome. *Blood* 1994; **83**: 2829–35.
3 Horning SJ. Natural history of and therapy for the indolent non-Hodgkin's lymphomas. *Semin Oncol* 1993; **20**: 75–88.
4 Solal-Celigny PH. Management of histologically indolent non-Hodgkin's lymphomas. *Baillieres Clin Hematol* 1996; **9**: 669–87.
5 Aisenberg AC. Coherent view of non-Hodgkin's lymphoma [review]. *Clin Oncol* 1995; **13**: 2656–75.
6 Reff M, Carner K, Chambers K *et al.* Depletion of B cells in vivo by a chimeric mouse human monoclonal antibody to CD20. *Blood* 1994; **83**: 435–45.
7 Taji H, Kagami Y, Okada Y *et al.* Inhibition of CD20-positive B lymphoma cell lines by IDEC-C2B8 anti-CD20 monoclonal antibody. *Jpn J Cancer Res* 1998; **89**: 748–56.
8 Demidem A, Lam T, Alas S, Hariharan K, Hanna N, Bonavida B. Chimeric anti-CD20 (IDEC-C2B8) monoclonal antibody sensitizes a B cell lymphoma cell line to cell killing by cytotoxic drugs. *Cancer Biother Radiopharm* 1997; **12**: 177–86.
9 McLaughlin P, Grillo-Lopez AJ, Link BK *et al.* Rituximab chimeric anti-CD20 monoclonal antibody therapy for relapsed indolent lymphoma: Half of patients respond to a four-dose treatment program. *J Clin Oncol* 1998; **16**: 2825–33.
10 Foran JM, Gupta RK, Cunningham D *et al.* A UK multicentre phase II study of rituximab (chimaeric anti-CD20 monoclonal antibody) in patients with follicular lymphoma, with PCR monitoring of molecular response. *Br J Haematol* 2000; **109**: 81–8.
11 Hainsworth JD, Burrism HA, Morrissey LH *et al.* Rituximab monoclonal antibody as initial systemic therapy for patients with low grade non-Hodgkin's lymphoma. *Blood* 2000; **95**: 3052–6.
12 Colombat P, Salles G, Brousse N *et al.* Rituximab (anti-CD20 monoclonal antibody) as single first-line therapy for patients with follicular lymphoma with a low tumor burden: Clinical and molecular evaluation. *Blood* 2001; **97**: 101–6.
13 Igarashi T, Kobayashi Y, Ogura M *et al.* Factors affecting toxicity, response and progression-free survival in relapsed patients with indolent B-cell lymphoma and mantle cell lymphoma treated with rituximab: a Japanese phase II study. *Ann Oncol* 2002; **13**: 928–43.
14 Czuczman MS, Grillo-Lopez AJ, White CA *et al.* Treatment of patients with low-grade B-cell lymphoma with the combination of chimeric anti-CD20 monoclonal antibody and CHOP chemotherapy. *J Clin Oncol* 1999; **17**: 268–76.
15 Czuczman MS, Weaver R, Alkuzweny B, Berlfein J, Grillo-Lopez AJ. Prolonged clinical and molecular remission in patients with low-grade or follicular non-Hodgkin's lymphoma treated with rituximab plus CHOP chemotherapy: 9-year follow-up. *J Clin Oncol* 2004; **22**: 4711–6.
16 Forstpointner R, Dreyling M, Repp R *et al.* The addition of rituximab to a combination of fludarabine, cyclophosphamide, mitoxantrone (FCM) significantly increases the response rate and prolongs survival as compared with FCM alone in patients with relapsed and refractory follicular and mantle cell lymphomas: results of a prospective randomized study of the German Low-Grade Lymphoma Study Group. *Blood* 2004; **104**: 3064–71.
17 Czuczman MS, Koryzna A, Mohr A *et al.* Rituximab in combination with fludarabine chemotherapy in low-grade or follicular lymphoma. *J Clin Oncol* 2005; **23**: 694–704.
18 Marcus R, Imrie K, Belch A *et al.* CVP chemotherapy plus rituximab compared with CVP as first-line treatment for advanced follicular lymphoma. *Blood* 2005; **105**: 1417–23.
19 Harris NL, Jaffe ES, Stein H *et al.* A revised European-American classification of lymphoid neoplasms: a proposal from the International Lymphoma Study Group. *Blood* 1994; **84**: 1361–92.
20 Carbone PP, Kaplan HS, Musshoff K, Smithers DW, Tubiana M. Report of the committee on Hodgkin's disease staging classification. *Cancer Res* 1971; **31**: 1860–1.
21 Oken MM, Creech RH, Tormey DC *et al.* Toxicity and response criteria of Eastern Cooperative Oncology Group. *Am J Clin Oncol* 1982; **5**: 649–55.

22 Hiddemann W. Current status and future perspectives in the treatment of low-grade non-Hodgkin's lymphomas. *Blood Rev* 1994; 8: 225–33.
23 Fleming TR. One sample multiple testing procedure for phase II clinical trials. *Biometrics* 1982; 38: 143–51.
24 Simon R, Thall PF, Ellenberg SS. New designs for the selection of treatments to be tested in randomized clinical trials. *Stat Med* 1994; 13: 417–29.
25 Tobinai K, Kobayashi Y, Narabayashi M *et al.* Feasibility and pharmacokinetic study of a chimeric anti-CD20 monoclonal antibody (IDEC-C2B8, rituximab) in relapsed B-cell lymphoma. *Ann Oncol* 1998; 9: 527–34.
26 Cheson BD, Horning SJ, Coiffier B *et al.* Report of an International Workshop to standardize response criteria for non-Hodgkin's lymphoma. *J Clin Oncol* 1999; 17: 1244–53.
27 Tobinai K, Kohno A, Shimada Y *et al.* Toxicity grading criteria of the Japan Clinical Oncology Group (JCOG). *Jpn J Clin Oncol* 1993; 23: 250–7.
28 Maloney DG, Grillo-Lopez AJ, Bodkin DJ *et al.* IDEC-C2B8: Results of a phase I multiple-dose trial in patients with relapsed non-Hodgkin's lymphoma. *J Clin Oncol* 1997; 15: 3266–74.
29 Solal-Celigny P, Roy P, Colombat P *et al.* Follicular lymphoma international prognostic index. *Blood* 2004; 104: 1258–65.
30 Freedman A, Gribben J, Neuberg D *et al.* High-dose therapy and autologous bone marrow transplantation in patients with follicular lymphoma during first remission. *Blood* 1996; 88: 2780–6.
31 Kimby E, Björkholm M, Gahrton G *et al.* Chlorambucil/prednisone vs. CHOP in symptomatic low-grade non-Hodgkin's lymphomas: a randomized trial from the Lymphoma Group of Central Sweden. *Ann Oncol* 1994; 5 (Suppl. 2): 67–71.
32 Maloney DG, Press OW, Braziel RM *et al.* A phase II trial of CHOP followed by rituximab chimeric monoclonal anti-CD20 antibody for treatment of newly diagnosed follicular non-Hodgkin's lymphoma: SWOG 9800 (Abstract). *Blood* 2001; 98: 843a.
33 Byrd JC, Peterson BL, Morrison VA *et al.* Randomized phase 2 study of fludarabine with concurrent versus sequential treatment with rituximab in symptomatic, untreated patients with B-cell chronic lymphocytic leukemia: results from Cancer and Leukemia Group B 9712 (CALGB 9712). *Blood* 2003; 101: 6–14.
34 Hainsworth JD, Litchy S, Burris HA III *et al.* Rituximab as first-line and maintenance therapy for patients with indolent non-Hodgkin's lymphoma. *J Clin Oncol* 2002; 20: 4261–7.
35 Ghielmini M, Schmitz SFH, Cogliatti SB *et al.* Prolonged treatment with rituximab in patients with follicular lymphoma significantly increases event-free survival and response duration compared with the standard weekly 4 schedule. *Blood* 2004; 103: 4416–23.

Appendix

Participating institutions and principal investigators of the IDEC-C2B8 Study Group included: Sapporo National Hospital (K. Aikawa, M. Nakata), Sapporo Hokuyu Hospital (M. Kasai, Y. Kiyama), Tochigi Cancer Center (Y. Kano, M. Akutsu), International Medical Center of Japan (A. Miwa, N. Takesako), National Cancer Center Hospital East (K. Itoh, T. Igarashi, K. Ishizawa), National Cancer Center Hospital (K. Tobinai, Y. Kobayashi, T. Watanabe), Tokyo Medical University (K. Ohyashiki, T. Tauchi), Tokai University School of Medicine (T. Hotta, T. Sasao), Hamamatsu University School of Medicine (K. Ohnishi), Aichi Cancer Center Hospital (Y. Morishima, M. Ogura, Y. Kagami), Nagoya University School of Medicine (T. Kinoshita, T. Murate, H. Nagai), Nagoya National Hospital (K. Tsushita, H. Ohashi), Mie University School of Medicine (S. Kageyama, M. Yamaguchi), Kyoto Prefectural University of Medicine (M. Taniwaki), Kyoto University School of Medicine (H. Ohno, T. Ishikawa), Shiga Medical Center for Adults (T. Suzuki), Center for Cardiovascular Diseases and Cancer, Osaka (A. Hiraoka, T. Karasuno), Hyogo Medical Center for Adults (T. Murayama), Hiroshima University School of Medicine (A. Sakai), National Kyushu Cancer Center (N. Uike), Nagasaki University School of Medicine (T. Maeda, K. Tsukasaki).

doi: 10.1111/j.1349-7006.2006.00173.x

Identification of subtype-specific genomic alterations in aggressive adult T-cell leukemia/lymphoma

Aya Oshiro, Hiroyuki Tagawa, Koichi Ohshima, Kennosuke Karube, Naokuni Uike, Yukie Tashiro, Atae Utsunomiya, Masato Masuda, Nobuyuki Takasu, Shigeo Nakamura, Yasuo Morishima, and Masao Seto

Aggressive adult T-cell leukemia/lymphoma (ATLL) such as acute and lymphoma types are fatal diseases with poor prognosis. Although these 2 subtypes feature different clinicopathologic characteristics, no detailed comparative analyses of genomic/genetic alterations have been reported. We performed array-based comparative genomic hybridization for 17 acute and 49 lymphoma cases as well as real-time quantitative polymerase chain reaction (PCR) to identify the target genes of recurrently amplified regions. Comparison of the genome profiles of acute and lymphoma types revealed that the lymphoma type had significantly more frequent gains at 1q, 2p, 4q, 7p, and 7q, and losses of 10p, 13q, 16q, and 18p, whereas the acute type showed a gain of 3/3p. Of the recurrent high-level amplifications found at 1p36, 6p25, 7p22, 7q, and 14q32 in the lymphoma type, we were able to demonstrate that *CARMA1* is a possible target gene of the 7p22 amplification for the lymphoma type but not for the acute type. Furthermore, we found *BCL11B* overexpression in the acute type regardless of the 14q32 gain/amplification, but no or low expression of the gene in the lymphoma type. These results suggest that acute and lymphoma types are genomically distinct subtypes, and thus may develop tumors via distinct genetic pathways. (Blood. 2006;107:4500-4507)

Introduction

Adult T-cell leukemia/lymphoma (ATLL) is a human T-lymphotropic virus type-I (HTLV-1)–mediated neoplasm.[1-3] ATLL develops tumors during a 40- to 70-year latency period from the time of HTLV-1 infection.[4] The results of statistical analysis suggest that additional genetic alterations are essential for viral integrated T cells to become malignant.[5]

Four major clinical subtypes—smoldering, chronic, acute, and lymphoma—have been identified.[6] The smoldering and chronic subtypes are characterized by an indolent clinical course, whereas the acute and lymphoma subtypes are aggressive and show poor prognosis, although their clinicopathologic features are clearly different. The acute type generally presents with hepatosplenomegaly, constitutional symptoms, elevated lactate dehydrogenase (LDH), and hypercalcemia,[7] but these are seen less often in the lymphoma type. The lymphoma type is characterized by prominent lymphoadenopathy without peripheral blood involvement, while the acute type is characterized by abnormal lymphocytes in peripheral blood and blood circulating in the whole body.[7] These differences suggest that these 2 subgroups develop tumors via distinct genetic pathways.

Two cytogenetic and 1 comparative genomic hybridization (CGH) study of genomic aberrations of ATLL have been reported.[8-10] The first 2 studies found that chromosome abnormalities of ATLL are complicated and occur more frequently in aggressive than in indolent ATLL. The third study, using conventional CGH analysis, showed that aggressive ATLL displayed more genomic gains and losses than the indolent type. However, despite these different clinicopathologic features of acute and lymphoma types, no comparative studies of the genomic aberrations of these subtypes have been reported. However, a comparative analysis of the genomic imbalances of these subtypes may provide important insights into the pathogenesis of aggressive ATLL.

To investigate the genomic aberrations of these subtypes, we performed high-resolution genome-wide array-based CGH (array CGH) for 17 patients with acute ATLL and 49 patients with lymphoma ATLL. For a further investigation of the relationship between genomic amplification and expression, we also performed quantitative real-time reverse transcription–polymerase chain reaction (RQ-PCR) to determine the target genes in some of the recurrent regions with high copy number gains.

From the Division of Molecular Medicine and Division of Hematology and Cell Therapy, Aichi Cancer Center Institute, Nagoya, Aichi; Department of Pathology, Kurume University School of Medicine, Kurume, Fukuoka; Department of Hematology, National Kyushu Cancer Center, Fukuoka; Department of Pathology, Imakiire General Hospital, Kagoshima; Department of Hematology, Imamura Bun-in Hospital, Kagoshima; Second Department of Internal Medicine, University Hospital, University of the Ryukyus, Nishihara, Okinawa; and Pathology/Clinical Laboratories, Nagoya University Hospital, Nagoya, Aichi, Japan.

Submitted September 22, 2005; accepted January 10, 2006. Prepublished online as *Blood* First Edition Paper, February 16, 2006; DOI 10.1182/blood-2005-09-3801.

Supported in part by a Grant-in-Aid from the Ministry of Health, Labor and Welfare; a Grant-in-Aid from the Ministry of Education, Culture, Sports, Science, and Technology; a Grant-in-Aid B2 and C from the Japan Society for the Promotion of Science; a Grant-in-Aid from the Foundation of Promotion of Cancer Research; a Grant-in-Aid for Cancer Research from the Princess Takamatsu Cancer Research Fund (03-23503); and a Grant-in-Aid from the China Japan Medical Association. The Wella Award from the Japan Leukemia Research Fund was awarded to M.S.

The online version of this article contains a data supplement.

Reprints: Masao Seto, 1-1 Kanokoden, Chikusa-ku Nagoya, 464-8681, Japan; e-mail: mseto@aichi-cc.jp.

The publication costs of this article were defrayed in part by page charge payment. Therefore, and solely to indicate this fact, this article is hereby marked "advertisement" in accordance with 18 U.S.C. section 1734.

Patients, materials, and methods

ATLL patients

Samples of peripheral blood and lymph nodes, together with clinical data, were obtained from 66 patients under a protocol approved by the Institutional Review Board of the Aichi Cancer Center. Informed consent was provided according to the Declaration of Helsinki. The patients were selected from those hospitalized between 1992 and 2004 at Fukuoka University School of Medicine, the University of the Ryukyus School of Medicine, Imamura-Bunin Hospital, and their affiliated hospitals. We identified 17 patients with acute ATLL and 49 patients with lymphoma type ATLL. The median survival from the time of diagnosis was 5.9 months for acute type and 12.5 months for lymphoma type. The diagnosis of ATLL was based on clinical features, hematologic characteristics, immunophenotype, the presence of serum antibodies to ATLL-associated antigens, and monoclonal integration of HTLV-I proviral DNA. The immunophenotype of the tumors was determined by immunohistochemistry for tissue sections and/or flow cytometry for cell suspensions (CD2, CD3, CD5, CD7, CD4, CD8, CD25, and CD45RO). Monoclonal integration of HTLV-I proviral DNA into ATLL cells was assayed by means of Southern blotting analysis. For the clinical subtypes of ATLL the classification by Shimoyama et al of acute, lymphoma, chronic, and smoldering types was adopted.[6]

Acute type. The acute type is characterized by a leukemic phase with a markedly elevated white blood cell count that consists of mainly abnormal lymphocytes known as "flower cells." The acute type is also characterized by hypercalcemia and/or a high LDH value (more than twice the upper limit of the normal range). Tumor specimens from all 17 patients, comprising 9 men and 8 women, were all obtained from the peripheral blood, which contained more than 60% leukemic cells (more than 10×10^9/L [10 000/μL]) at the time of diagnosis. The median age of the patients was 57 years (range, 44-78 years); 16 patients had elevated LDH, 9 had elevated serum calcium levels, and 9 had a poor performance status (Table 1).

Lymphoma type. The lymphoma type is characterized by prominent lymphoadenopathy without peripheral blood involvement. Tumor specimens were obtained from 26 men and 23 women whose median age was 64 years old (range, 36-85 years). No leukemic cells were recognized in the peripheral blood at the time of diagnosis (Table 1).

Table 1. Characteristics of ATLL patients and their clinical features based on diagnostic criteria (n = 66)

Characteristic	Acute type	Lymphoma type
No. of patients	17	49
Median age, y (range)	57 (44-78)	64 (36-85)
Sex, no. male (%)	9 (53)	26 (53)
Performance status, no. (%)		
0-2	8 (47)	ND
Greater than 2	9 (53)	ND
Nodal involvement, no. (%)	7 (41)	49 (100)
Hepatosplenomegaly, no. (%)	6 (35)	ND
Cell type*	Peripheral blood	Lymph node
Flower cells†	+	−
Elevated WBC count‡, no. (%)	17 (100)	ND
LDH level, no. (%)		
Normal	1 (6)	ND
Elevated	16 (94)	ND
Ca level, no. (%)		
Normal	8 (47)	ND
Elevated	9 (53)	ND

ND indicates not determined; +, present; −, absent.

*Cell types from which the DNA was extracted: peripheral blood for acute type and lymph node for lymphoma type.

†Flower cells were observed in peripheral blood in all patients with acute-type ATLL, and in none of the patients with lymphoma-type ATLL.

‡Elevated WBC count defined as more than 10×10^9/L (10 000/μL).

DNA and RNA samples

High molecular weight DNA was extracted from lymph nodes and peripheral blood by using standard proteinase K/RNase treatment and phenol-chloroform extraction. DNA and RNA samples were extracted from frozen tissue. Normal DNA was obtained from the blood of healthy male donors. RNA was prepared from lymph nodes and peripheral blood by homogenization in guanidinium thiocyanate and centrifugation through cesium chloride.

Southern blotting for the HTLV-1 genome

Monoclonal integration of HTLV-I provial DNA into ATLL cells was demonstrated by Southern blotting analysis. Briefly, high-molecular-weight DNA was extracted from mononuclear cells (MNCs). DNA samples (5 μg) were digested with *Eco*RI and size-fractionated on 0.75% agarose gels. They were then electrotransferred onto a nitrocellulose membrane and hybridized to randomly primed ^{32}P-labeled DNA probes specific for HTLV-I. Thereafter, the blots were washed at appropriate stringency and visualized by autoradiography.[11]

Array-based CGH

The array consisted of 2304 BAC and PAC clones, covering the human genome at a resolution of roughly 1.3 Mb, from libraries RP11 and RP13 for BAC clones, and RP1, RP3, RP4 and RP5 for PAC clones. BAC and PAC clones were selected from the information from the National Center for Biotechnology Information (NCBI; http://www.ncbi.nlm.nih.gov/), Ensembl Genome Data Resources (http://www.ensembl.org/), and the University of California at Santa Cruz (UCSC) genome Bioinfomatics, and obtained from the BACPAC Resource Center at the Children's Hospital (Oakland Research Institute, Oakland, CA). Clones were ordered from chromosomes 1 to 22 and X within each chromosome on the basis of Ensembl Genome Data Resources from the Sanger Center Institute (February 2005 version). The locations of all the clones used for array CGH were confirmed by fluorescence in situ hybridization (FISH). For the array, 10 simultaneous hybridizations of healthy male versus healthy male were performed to define the normal variation for the $\log_2$ ratio. A total of 113 clones with less than 10% of the mean fluorescence intensity of all the clones, with the most extreme average test-over-reference ratio deviations from 1.0 and with the largest standard deviation in this set of normal controls excluded from further analyses.

A total of 2235 clones (covering 2988 Mb, 1.3 Mb of resolution) were therefore subjected to further analysis. Since more than 96% of the measured fluorescence $\log_2$ ratio values at each spot (2×2235 clones) ranged from +0.2 to −0.2, the thresholds for the $\log_2$ ratio of gains and losses were set at $\log_2$ ratios of +0.2 and −0.2, respectively. Regions of low-level gain/amplification were defined as $\log_2$ ratio +0.2 to +1.0; those suspected of containing a heterozygous loss/deletion were defined as $\log_2$ ratio −1.0 to −0.2, and those showing high-level gain/amplification as $\log_2$ ratio greater than +1.0, and those suspected of containing a homozygous losses/deletion as $\log_2$ ratio less than −1.0.[12-14]

Real-time quantitative polymerase chain reaction

Expression levels of mRNA were measured by means of real-time fluorescence detection using a previously described method.[15] Briefly, the primers of *CARMA1* were sense: 5′-CATTCTACATACCAAGGGGC-3′ and antisense: 5′-ATCTGCTGCTGCAGCTTGAT-3′; the primers of *BCL11b* were sense: 5′-CAAGCAGGAGAACATTGCAG-3′ and antisense: 5′-AGTGATCACGGATGAGTGAG-3′; the primers of IRF4 were sense: 5′-AGAAGAGCATCTTCCGCATC-3′ and antisense: 5′-TGCTCTTGTTCAAAGCGCAC-3′. The real-time PCR using SYBR Green I (Takara Bio, Tokyo, Japan) and the primers was performed with a Smart Cycler System (Takara Bio) according to the manufacturer's protocol. *G6PDH* served as an endogenous control, while the expression levels of CARMA1 mRNA in each sample were normalized on the basis of the corresponding *G6PDH* content and recorded as relative expression levels. All the experiments were performed in duplicate.

Statistical analysis

To analyze genomic regions for statistical differences between the 2 patient groups, the data set was constructed as follows. Genomic alterations were defined by a $\log_2$ ratio threshold of +0.2 for copy number gain, and of −0.2 for copy number loss. Gained clones ($\log_2$ ratio > +0.2) were inputted as "1" versus no-gained clones ($\log_2$ ratio < +0.2) as "0" in an Excel template for each case (Microsoft, Redmond, WA). Similarly, lost clones ($\log_2$ ratio < −0.2) were inputted as "1" versus no-lost clones ($\log_2$ ratio > −0.2) as "0" in another Excel template. Cases showing genomic gain or loss were counted with an Excel template for each single clone (2235 clones in all) in the acute or the lymphoma group. Data analyses were then performed for the comparison of frequencies of gain or loss for each single clone between the acute and lymphoma groups (2235 tests each for gain and loss, 4470 tests in all). Fisher exact test for probability was used for the former analysis. The P value for screening of candidate clones was less than .05 for every analysis. When a candidate clone was identified, the clone's continuity with the subsequent clones was evaluated. In cases where the nth clone and subsequent k clones ($k \geq 0$) were found to be candidate clones, the P value for continual association was calculated as $\prod_{i=n}^{n+k} p_i$ under the assumption that each clone is independent throughout the entire genome. As we applied multiple tests (4470 tests maximum), the conventional Bonferroni procedure was applied to define the alfa-error for the final conclusion.[16] Therefore, we defined a $\prod_{i=n}^{n+k} p_i$ value of less than 0.05 per 4470 ($= 1 \times 10^{-5}$) as statistically significant.

The Mann-Whitney U test was used for detecting significant differences in expression levels of *IRF4* (6p25), *CARMA1* (7p22), and *BCL11B* (14q32) in groups with and without the genomic amplifications. All the statistical analyses were conducted with the STATA version 8 statistical package (StataCorp, College Station, TX).

Results

Detection of genomic imbalances in ATLL

Representative individual examples of the high-resolution analysis of 2 patient samples are shown in Figure S1 (see the Supplemental Figure link at the top of the online article, at the *Blood* website). Array CGH detected both small and large chromosome areas of gains and deletions as well as clear amplification and deletion borders. Gains and losses of genetic material obtained from 66 patients (49 with lymphoma ATLL and 17 with acute ATLL) were subjected to data analysis.

Genomic imbalances in acute type. Of the 17 patients analyzed, 1 sample did not show any copy number change. The entire tumor set, including the case without any genomic alterations characteristic of the acute type, involved average copy number gains of 221 Mb and 4.2 regions, and average copy number losses of 133 Mb and 4.5 regions (Table 2). Regions of recurrent (> 20%) gain were detected on chromosomes 3, 8p11.21-8q13.1, 8q24.21-24.23, 9p24.3-24.1, 9q33.3-34.3, 14q31.1-32.33, and X, and regions of recurrent loss on chromosomes 2q37.1-37.3, 4q21.1-24, 6q14.1, 9q21.12-31.2, 17p13.1, and 19q13.31-13.2 (Figures 1A,2A).

Table 2. Copy number alterations of ATLL

	Acute type	Lymphoma type
Copy number gain*		
Average genome size, Mb	221.5	356.46
Average % of the genome	7.5	12.2
Average no. of regions	4.18	9.69
Copy number loss*		
Average genome size, Mb	133.0	274.3
Average % of the genome	4.5	9.3
Average no. of regions	4.5	9.75

For acute-type ATLL, n = 17; for lymphoma-type ATLL, n = 49.
*Copy number change of X chromosome was excluded.

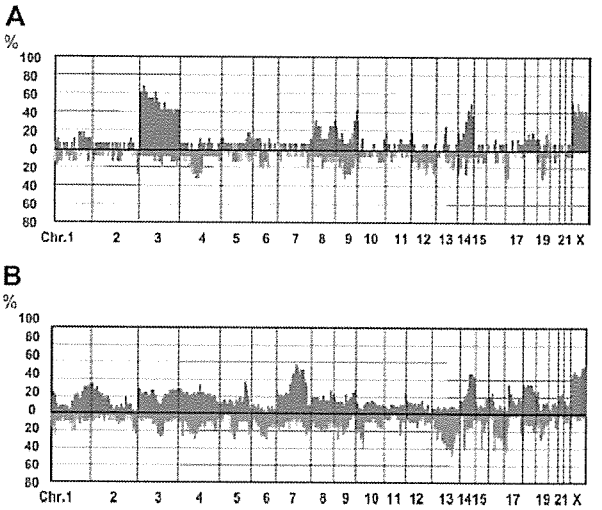

Figure 1. Genome-wide frequency of genomic imbalance in acute and lymphoma type ATLL. Horizontal lines indicate 2235 BAC/PAC clones listed in order from chromosomes 1 to 22 and X. Within each chromosome, clones are shown in order from the p to the q telomere in accordance with information from the Ensembl Genome Data Resources of the Sanger Center Institute (February 2005 version). Vertical lines indicate frequency (%) of gains and losses. (A) Acute type (17 patients). (B) Lymphoma type (49 patients). The green area represents genomic gain; red region, genomic loss.

Genomic imbalances in lymphoma type. Gains and losses of genetic materials obtained from 49 patient samples of the lymphoma type were subjected to data analysis. All of the cases demonstrated genomic aberrations. The entire tumor set involved average copy number gains of 356 Mb and 9.7 regions and average copy number losses of 274 Mb and 9.8 regions (Table 2). Regions of recurrent (> 20%) gain were detected on chromosomes 1p36.23-36.21, 1p21.3-23.3, 1p25.2-1q44, 2p25.1-22.3, 2p2.1-21, 3p26.3-q12.3, 3q25.2-29, 4p16.3-q12, 4q13-34.1, 6p25.3-24.1, 7p22.3-15.2, 7p14.3-14.2, 7p13-q36.3, 8q21.3-22.2, 8q24.22-24.21, 9p24.2-24.1, 9q34.3, 14q31.1-32.33, 18cen-23q, 21q21-22.2, and X, and losses at 1p31.2-12, 2q36.1-37.3, 3q13.13-24, 4q13.2-22.3, 5q15-23.1, 6q14.1-22.31, 8p23.3-21.2, 8q21.13, 9p21.3, 9q21.12-21.33, 10p15.3-cen., 13q12.3-34, 14q11.2-21.1, 16cen-16q24.1, 17p13.3-12, 18p11.32-cen, and 19p13.11-13.32 (Figures 1B,2B).

Comparison of genomic profiles of acute and lymphoma types

A comparative analysis of the differences in genomic frequencies between acute and lymphoma types identified several common regions for these 2 subtypes. The common regions of gains were found on 3p36-q12, 3q25-29, 8q24, 9p24, 9q34, and 14q32, and those of losses on 2q37, 4q21, 6q14, 9p21, 9q21, 17p13.1, and 19q13. Statistically significant differences were a gain of 3p26-q26 for the acute type and gains at 1q22-23, 1q41-44, 2p25, 4q21-22, 4q26-27, 7p22, and 7q11-36, and losses of 10p12, 13q21-32, 16q21-22, and 18p11 for the lymphoma type. The regions characteristic of each type as determined are listed in Table 3.

Recurrent genomic amplifications, homozygous losses, and candidate target genes

Recurrent regions (≥ 2 patients) of high-level amplification ($\log_2$ ratio > +1.0) were found at 1p36, 6p25, 7p22.2, 7q21-q22, 7q31-q36, and 14q32 (Table 4) in the lymphoma-type samples, and

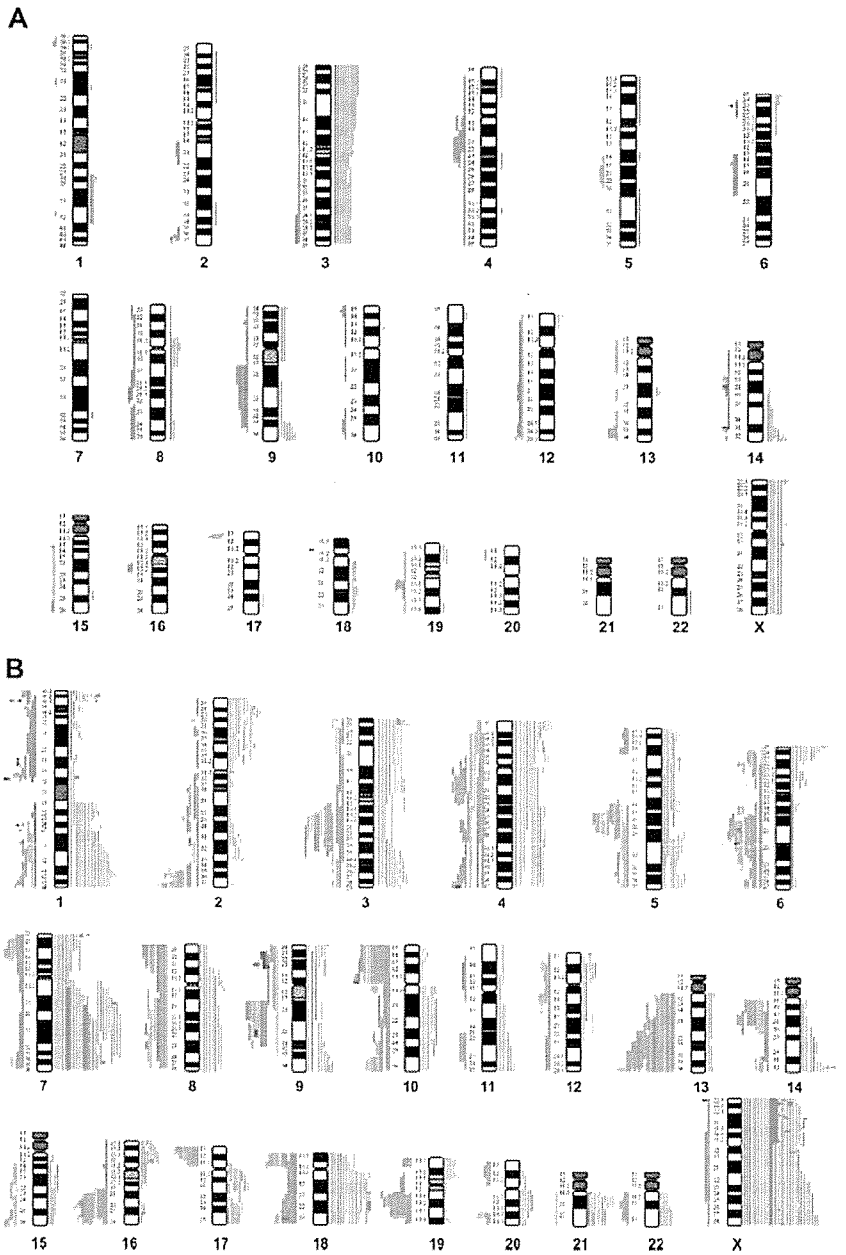

Figure 2. Ideograms of acute and lymphoma types of ATLL. Summary of the chromosomal imbalance detected in 17 acute-type patients (A) and 49 lymphoma-type patients (B). Lines on the left (red) of the ideograms indicate losses, and those on the right (green) indicate gains. Red rectangles on the left represent homozygous losses ($\log_2$ ratio < -1.0), and green rectangles on the right represent high copy number gains ($\log_2$ ratio $> +1.0$).

no recurrent amplifications or homozygous losses in the acute type. In an attempt to identify target genes in the high-level amplification regions, those with amplification detected by a single BAC clone were further analyzed (Figure 3). The 3 regions containing candidate genes that have been implicated in lymphoid malignancies were *IRF4* at 6p25.3, *CARMA1* at 7p22.2, and *BCL11B* at 14q32 (2 patients each).[17-19] Candidate target genes of the other regions (eg, 1p36, 7q21-q22, and 7q31-q36) are currently being investigated.

A recurrent region of homozygous loss ($\log_2$ ratio < -1.0) was found at 9p21.3. As shown in Table 4, the most frequently detected clone of homozygous loss at 9p21.3 was RP11-149I2 (2 cases: D1679 and D1687), which contains the *CDKN2A* and *CDKN2B* tumor suppressor genes. Other recurrent regions of homozygous loss are suspected to be 6q21 and 13q32.

Real-time quantitative PCR analysis for *IRF4*, *CARMA1*, and *BCL11B*

IRF4, *CARMA1*, and *BCL11B* of the 6p25, 7p22, and 14q32 regions were examined for their potential as candidate target genes. These genes are included in the BAC clones with high copy number gains (RP11-498D18, *CARMA1*; and RP11-233K4, *IRF4*) or located very close to such BAC clone (*BCL11B*; 300 kb telomeric to RP11-1127D7). To identify the candidate target genes for these genomic regions, we performed RQ-PCR analysis for 21 patients either with or without this gain/amplification. Although the statistical power of this analysis is limited because of the small number of cases, the expression levels of *CARMA1* of the patients with copy number gains at 7p22 were significantly higher than of those without (Mann-Whitney U test, $P = .045$). However, high expression of *CARMA1* was found in the acute type regardless of the 7p22

Table 3. Regions of genomic alterations characteristic of acute or lymphoma types

Chromosome band*	Megabases	Acute type†	Lymphoma type†
Gain			
1q22-23.1	3	0	11
1q41-44	29.3	0	12-17
2p25	3.1	0	10-13
3p26.3-q26.2	0.2-170.85	6-11‡	4-14
4q21.1-22.1	76.5-92.2	0	10-12
4q26-27	115.7-120.3	0	10-12
7p22.2-22.3	0.5-3.7	0	10-13
7q11.23-7q36.3	76.2-156.9	0-1	15-28
Loss			
10p12.31-12.1	20-28.3	0-1	11-15
13q21.1-q32.1	49.45-91	0-1	10-20
16q21-q22.2	9.6-73.1	0	10-13
18p11.22	8.7-10.1	0	12

For acute-type ATLL, n = 17; for lymphoma-type ATLL, n = 49.

*Regions are listed that showed significant differences in frequency between acute and lymphoma types.

†Number of cases with genomic alterations.

‡Characteristic region of acute type.

gain/amplification. We therefore concluded that the *CARMA1* gene is a target for 7p22 genomic amplification in the lymphoma type but not in the acute type. Repeated experiments showed similar results with a variance of less than 5%; representative data are shown in Figure 4.

With regard to the 14q32 region, RQ-PCR for *BCL11B* failed to demonstrate high-level expression in the cases with high copy number gains, indicating that *BCL11B* is not a candidate gene for the 14q32 region of the lymphoma type (Figure 5). Interestingly, high-level expression of *BCL11B* was noted in the acute type lacking genomic amplification. Various levels of *IRF4* expression were observed regardless of genomic gains, indicating that *IRF4* is not a likely candidate gene of this region (data not shown).

Discussion

ATLL is categorized as a single-disease entity; the neoplasm originated from HTLV-I–infected T cells in the World Health Organization (WHO) classification, although the disease is comprised of 4 subtypes—smoldering, chronic, lymphoma, and acute—which reveal distinct clinicopathologic features.[7]

Previous cytogenetic analysis of ATLL indicated that this disease is characterized by complicated and miscellaneous genomic alterations. Kamada et al studied 107 patients with ATLL and reported recurrent cytogenetic abnormalities, including gains of chromosomes 3, 7, and 21, and various losses.[8] Tsukasaki et al analyzed 46 patients with aggressive ATLL (acute and lymphoma types) by means of chromosomal CGH and reported frequent genomic gains at 3p, 7q, and 14q, and losses at 6q and 13q.[10] They also demonstrated that aggressive ATLL featured significantly more frequent genomic aberrations than did indolent types such as

Table 4. List of BAC/PAC clones showing recurrent high copy number gains and homozygous losses in lymphoma type

Clone name*	Cytogenetic position	Gain/loss, no. patients†	Amplification/homozygous loss, no. patients‡	Gene§
Gain				
RP3-510D11	1p36.22	12	2	*H6PD, LOC440558*
RP5-888M10	1p36.21	11	2	*VPS13D*
RP5-1177E19	1p36.21	9	2	*PRDM2*
RP11-233K4	6p25.3	18	2	*IRF4*‖
RP11-498D18	7p22.2	12	2	*CARMA1*,‖ *GNA12*
RP5-911H5	7q21.2	22	2	*ANKIB1*
RP11-736C20	7q21.2	23	2	*CALCR*
RP11-148A10	7q22.2	26	2	*LHFPL3*
RP11-77E2	7q22.3	25	2	*DLD, LAMB1, LAMB4*
RP11-573B16	7q31.1	25	2	—
RP11-9C22	7q31.33	25	2	*SND1*
RP11-66F23	7q31.33	24	2	*NYD-SP18, CALU, OPN1SW, DKFZP434G156, FLNC, ATP6V1F, LOC375616*
RP11-35B6	7q31.33	24	2	*KIAA0828, FAM40B*
RP11-233L24	7q33	21	2	—
RP4-659J6	7q33	24	2	*ZC3HDC1, KIAA1718*
RP11-188A12	7q33	20	2	—
RP11-796I2	7q35	17	2	*PRKAG2, LOC441301, GALNTL5*
RP11-476H24	7q36.2	18	2	*DPP6*
RP11-691F21	7q36.3	18	2	*LOC285889*
RP11-452C13	7q36.3	16	2	*PTPRN2*
RP11-1127D7	14q32.2	21	2	*FLJ25773,*¶ *RPL3P4,*¶ *BCL11B*‖¶
Loss				
RP1-101M23	6q21	12	2	*PRDM1*
RP11-149I2	9p21.3	14	2	*MTAP, CDKN2A,*‖ *CDKN2B,*‖ *NSGX*
RP11-214L15	9p21.3	7	2	—
RP11-468C2	9p21.3	5	2	—
RP11-461N23	13q32.1	24	2	*GPR18, PHGDHL1, EBI2*

*List of BAC clones from p telomere to q telomere are listed for each chromosome number.

†Gain was defined as $\log_2$ ratio +0.2 to +1.0, loss as $\log_2$ ratio −1.0 to −0.2.

‡Amplification was defined as $\log_2$ ratio greater than +1.0 and homozygous loss as $\log_2$ ratio less than −1.0.

§All of the genes located on the BAC/PAC clones. If there were any oncogenes in the clone adjacent to the amplified or lost one, they were listed.

‖The names of genes located in the BAC clones adjacent to RP11-1127D7 are listed. BCL11B is 0.3 Mb telomeric to RP11-1127D7.

¶These genes have been implicated in lymphoid malignancies.[17-21]

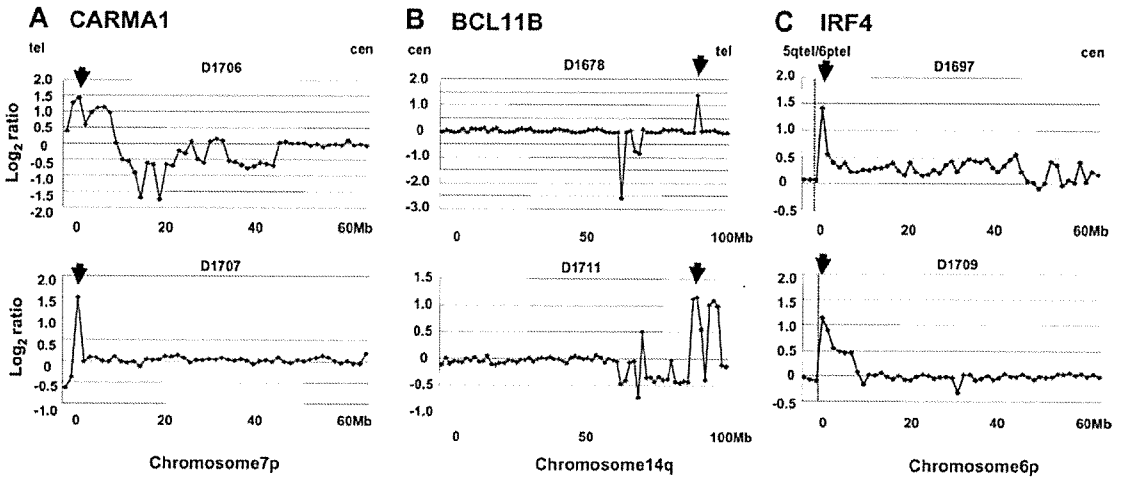

Figure 3. Individual genome profiles of amplification at 6p, 7p, and 14q. Although there were only 2 lymphoma-type cases with high copy number gains, 3 regions are shown because they contained genes implicated in lymphomagenesis. No high copy number gains were found in acute-type cases. (A) Individual genome profiles of high copy number gains at 7p22.2 for 2 patients (D1706 and D1707). Horizontal lines indicate the megabase (Mb) from the 7p telomere to the centromere, and vertical lines show the $\log_2$ ratio. Spots are ordered contiguously from the p telomere to the centromere, with an average resolution of 1.3 Mb. The threshold for gain and loss was defined as a $\log_2$ ratio of +0.2 and −0.2, respectively. The arrow above each graph represents the highest peak at 7p22.2. RP11-498D18 located in the peak contains *CARMA1*. (B) Individual genome profiles of high copy number gains at 14q32 for 2 patients (D1678 and D1711). Spots are ordered contiguously from the 14q centromere to the 14q telomere. The arrow above each graph represents the highest peak at 14q32. RP11-1127D7 located in the peak is 0.3 Mb telomeric to *BCL11B*. (C) Individual genome profiles of high copy number gains at 6p25 for 2 patients (D1697 and D1709). Spots are ordered contiguously from the 6p telomere to the 6p centromere. The arrow above each graph represents the highest peak at 6p25. RP11-233K4 located in the peak contains *IRF4*. Based on information from the Ensembl Genome Data Resources of the Sanger Center Institute and NCBI. Vertical dotted lines represent the boundary between 5q and 6q telomeres.

chronic and smoldering. However, they did not perform a comparative analysis of genomic alterations in acute and lymphoma types. Our study showed that gain at chromosome 3p26-q26 was a frequent genomic aberration of the acute type, while gain at 7q and loss at 13q were characteristic of the lymphoma type.

The common genomic alterations may represent the common oncogenic changes for both types, while differences in their genome profiles may represent different clinical phenotypes. The loss of 9p21 was detected in 20% of patients with acute ATLL and 33% of patients with lymphoma ATLL. The loss of 9p21, which harbors the *CDKN2A* and *CDKN2B* tumor suppressor gene, has been frequently found in aggressive ATLL but not infrequently in indolent types.[20,21] This suggests that deregulation of tumor suppressor genes such as *CDKN2A* and *CDKN2B* is likely to lead to the transition from indolent to aggressive type. Gain of the 3p26-q26 region is characteristic of the acute type of ATLL, which in turn is characterized by a leukemic phase with flower cells. Recently, it has been demonstrated that phosphatidylinositol 3-kinase, catalytic, beta *(PIK3CB2)* located at 3q22.3 is associated with flower cell formation and the cellular proliferation of ATLL.[22] It is tempting to speculate that the gain of 3p26-q26 results in aberrant

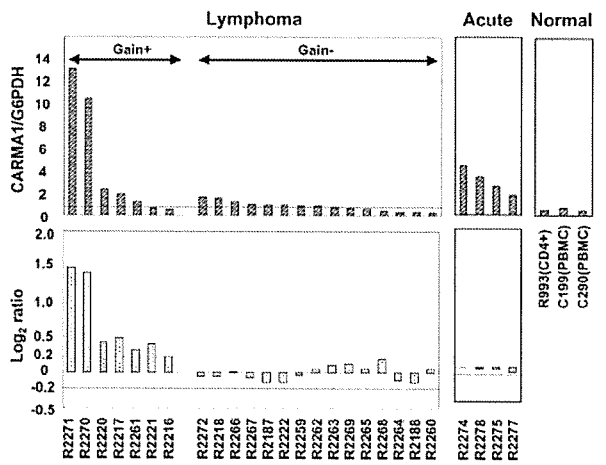

Figure 4. RQ-PCR for *CARMA1* and correlation of genomic amplification. RQ-PCR was used to detect the expression level of *CARMA1* in ATLL patients with or without 7p22 gain/amplification. Twenty lymphoma-type cases were divided into 2 groups, 1 group with copy number gain/amplification (gain +) and the other group without any copy number change (gain −). The top panels show expression levels of *CARMA1* determined by RQ-PCR, while the bottom panels indicate genomic profiles determined by array CGH. The horizontal dotted line in the top left panel in the gain group indicates the mean value (0.603) of the expression level (SD, 0.312). Four patients with acute-type ATLL are represented in the center panels. For comparison, 1 sample of $CD4^+$ T cells isolated from peripheral blood mononuclear cells (PBMCs) and 2 samples of PBMCs were examined by RQ-PCR (right panels).

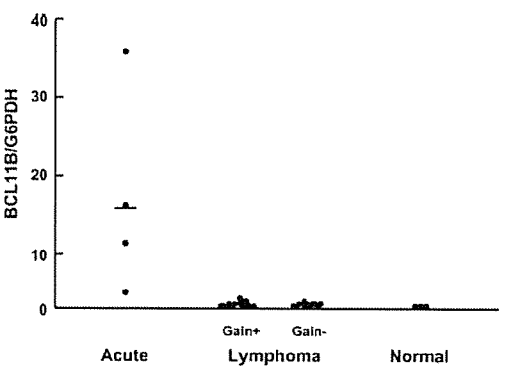

Figure 5. RQ-PCR for *BCL11B* in acute and lymphoma types. RQ-PCR was used to detect expression levels of *BCL11B* in acute and lymphoma types of ATLL. Four patients with acute-type ATLL showed high levels of *BCL11B* expression, although none of them showed any genomic change at RP11-1127D7. The horizontal bar indicates the mean expression level (16.32). Eleven patients with lymphoma-type ATLL with gains at RP11-1127D7 and 10 patients without any genomic change are also shown. None of these patients showed any significant level of expression. For comparison, *BCL11B* expression was examined in 1 $CD4^+$ PBMC sample and 2 PBMC samples (Normal). The 4 acute-type patients showed significantly higher expression than did the 21 lymphoma-type patients. (Acute type versus lymphoma type with 14q32 gain [+]: Mann-Whitney *U* test, $P = .002$; acute type versus lymphoma gain [−]: Mann-Whitney *U* test, $P = .005$).